



High-resolution imaging of bacterial spatial organization with vertical cell imaging by nanostructured immobilization (VerCINI)

Kevin D. Whitley^{1,2}✉, Stuart Middlemiss¹, Calum Jukes¹, Cees Dekker^{1,2} and Séamus Holden¹✉

Light microscopy is indispensable for analysis of bacterial spatial organization, yet the sizes and shapes of bacterial cells pose unique challenges to imaging. Bacterial cells are not much larger than the diffraction limit of visible light, and many species have cylindrical shapes and so lie flat on microscope coverslips, yielding low-resolution images when observing their short axes. In this protocol, we describe a pair of recently developed methods named VerCINI (vertical cell imaging by nanostructured immobilization) and μVerCINI (microfluidic VerCINI) that greatly increase spatial resolution and image quality for microscopy of the short axes of bacteria. The concept behind both methods is that cells are imaged while confined vertically inside cell traps made from a nanofabricated mold. The mold is a patterned silicon wafer produced in a cleanroom facility using electron-beam lithography and deep reactive ion etching, which takes ~3 h for fabrication and ~12 h for surface passivation. After obtaining a mold, the entire process of making cell traps, imaging cells and processing images can take ~2–12 h, depending on the experiment. VerCINI and μVerCINI are ideal for imaging any process along the short axes of bacterial cells, as they provide high-resolution images without any special requirements for fluorophores or imaging modalities, and can readily be combined with other imaging methods (e.g., STORM). VerCINI can easily be incorporated into existing projects by researchers with expertise in bacteriology and microscopy. Nanofabrication can be either done in-house, requiring specialist facilities, or outsourced based on this protocol.

Introduction

Although long underappreciated as amorphous sacks of enzymes, it is now clear that bacterial cells are highly spatially organized. How bacterial proteins dynamically organize and remodel large cellular structures such as the cell wall or the chromosome is a central question in bacteriology. However, imaging cellular spatial organization and dynamics inside bacteria by light microscopy is challenging for several reasons. First, bacteria are very small, with a typical diameter of 1 µm, not much larger than the 250 nm diffraction limit of visible light. Second, most bacteria are not spherically symmetric, but exist in a wide range of shapes, including rods and ovoids. During imaging, nonspherical bacteria are usually immobilized flat on a microscope coverslip, with their long axes parallel to the imaging plane and their short axes orthogonal to the imaging plane (Fig. 1a, top). Imaging structure and dynamics along the short axes is therefore difficult, both due to a large amount of background signal from out-of-focus light and the fact that axial resolution is generally lower than lateral resolution (~250 nm lateral versus 550 nm axial resolution¹).

This is especially problematic when one considers that many bacterial processes occur, or are organized, along these shorter axes. For example, the peptidoglycan cell wall is primarily synthesized circumferentially around the cell during vegetative growth in many bacteria^{2–4}. Similarly, when cells divide, their division machinery moves circumferentially around the cell septum to progressively synthesize the cell septum inwards^{5,6}. When cells have divided, what was once the division plane becomes two daughter cell poles, which then also exist along the short axes of the cells. A large number of proteins localize specifically to the cell poles in rod-shaped bacteria that carry out a wide variety of functions, such as chemotaxis, motility, adhesion, virulence, chromosome organization, cell-cycle regulation and secretion^{7–11}. A wealth of information on all these systems has been obtained

¹Centre for Bacterial Cell Biology, Biosciences Institute, Newcastle University, Newcastle upon Tyne, UK. ²Department of Bionanoscience, Kavli Institute of Nanoscience Delft, Delft University of Technology, Delft, the Netherlands. ✉e-mail: kevin.whitley@ncl.ac.uk; seamus.holden@ncl.ac.uk

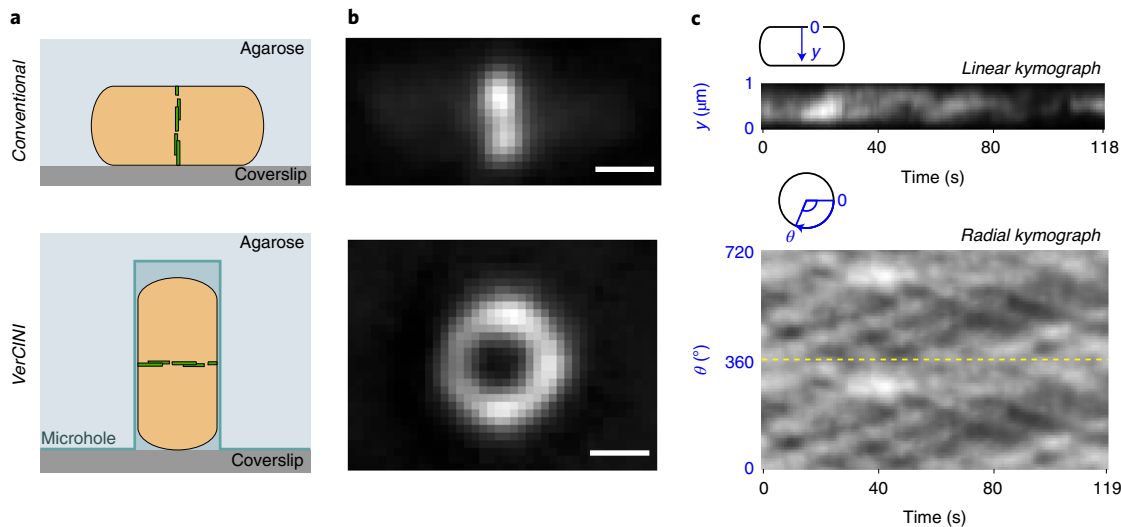


Fig. 1 | Concept of VerCINI and comparison with conventional imaging of division protein dynamics. **a**, Schematics comparing conventional imaging and VerCINI to image division protein dynamics in rod-shaped cells. Division rings depicted as green dashed lines. Top: a cell lying horizontally under an agarose pad, with its division ring orthogonal to the microscope coverslip. Bottom: a cell confined vertically in an agarose microhole, with its division ring parallel to the microscope coverslip. **b**, Representative images of *B. subtilis* cells expressing labeled FtsZ. Top: TIRF illumination of a cell expressing mNeonGreen-FtsZ ectopically from an inducible promoter (strain bWM4³⁹). The bottom of the division ring appears as a line across mid-cell. Bottom: HILO illumination of a cell expressing FtsZ-GFP as a sole copy of FtsZ from the native locus (strain SH130¹²). The full division ring appears as a circle. Scale bars, 500 nm. **c**, Kymographs of FtsZ treadmilling dynamics from cells in **b**. Top: kymograph of mNeonGreen-FtsZ treadmilling dynamics from 0 to 1 μ m across the short axis of the cell. Diagonal lines show directional motion across the short axis of the cell. Bottom: kymograph of FtsZ-GFP treadmilling dynamics around the cell circumference. Two full revolutions around the cell (0–720°) are plotted side-by-side to resolve filament trajectories that cross 0°/360°, separated by a yellow dotted line. Diagonal lines show directional motion around the full circumference of the cell. Raw data from ref. ¹².

from microscopy in recent years, but a major limitation remains that the horizontal orientation of cells is far from optimal for imaging these systems.

To address this problem we developed a method, termed vertical cell imaging by nanostructured immobilization (VerCINI), that enables high-resolution light microscopy of any process organized along the short axes of bacterial cells by orienting cells vertically in nanofabricated cell traps^{5,12,13}. We also developed a method for high-resolution imaging of the short axes of bacteria during fluid exchange termed microfluidic VerCINI (μ VerCINI)¹². Here we provide a detailed practical guide to implementing both VerCINI and μ VerCINI. We first give a general overview of the VerCINI method and its applications. We provide detailed workflows for all aspects of VerCINI and μ VerCINI, from nanofabrication of micropillar arrays to acquisition and analysis of microscopy data. We provide rationales for the procedures described and include tips from our own experience in developing and using the methods to assist interested researchers. We also provide quantitative analysis of critical steps in the method to support troubleshooting and to enable future extensions and adaptations of the technique to new applications. By following the procedures described, this article should allow interested researchers to easily apply VerCINI to their own research.

Development of the protocol

We recently developed two methods that enable high-resolution imaging of bacteria along their short axes by orienting them vertically in nanofabricated cell traps^{5,12,13}. In the first method, VerCINI, cells are confined in nanofabricated ‘microhole’ arrays formed in an agarose pad such that the short axes of the cell are aligned to the microscope imaging plane, allowing much higher resolution of images of the cell short axis than is possible with conventional immobilization (Fig. 1a and Fig. 2a, bottom). In the second method, μ VerCINI, the microhole arrays are open-topped, and the vertically trapped cells are confined within a microfluidic chamber to enable rapid solution exchange and chemical perturbation (Fig. 3a). Both methods were originally developed to trap rod-shaped bacterial cells, which include the majority of model systems (e.g., *Bacillus subtilis* and *Escherichia coli*) and many human pathogens (e.g., *Mycobacterium tuberculosis*). However, they are suitable for any cells with cylindrical symmetry, which also includes ovococcal species such as the human pathogen *Streptococcus pneumoniae*.

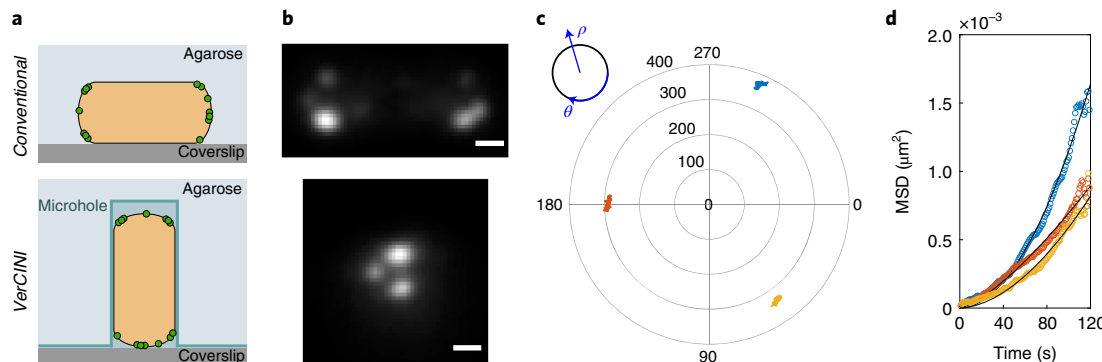


Fig. 2 | Concept of VerCINI and demonstration to conventional imaging of polar protein dynamics. **a**, Schematics comparing conventional imaging and VerCINI to image polar proteins in rod-shaped cells. Polar proteins are depicted as green circles. Top: a cell lying horizontally under an agarose pad, with its poles orthogonal to the microscope coverslip. Bottom: a cell confined vertically in an agarose microhole, with its poles parallel to the microscope coverslip. **b**, Representative images of *B. subtilis* cells expressing TlpA-mGFP ectopically from an inducible promoter (strain HS48²²; Supplementary Methods). Top: using conventional imaging with HiLO illumination, the proteins appear as unresolved blobs at cell poles. Bottom: using VerCINI with TIRF illumination, the proteins appear in several discrete clusters. Scale bars, 500 nm. **c**, Polar plot showing the motion of TlpA-mGFP clusters from the VerCINI imaging in **b**. Motion of clusters tracked using TrackMate⁴⁰. **d**, Mean squared displacements of clusters in **c** for different time intervals (circles; colors correspond to those in **c**) with fits to generalized diffusion equation $\langle r^2(t) \rangle = K_\alpha t^\alpha$. (black lines).

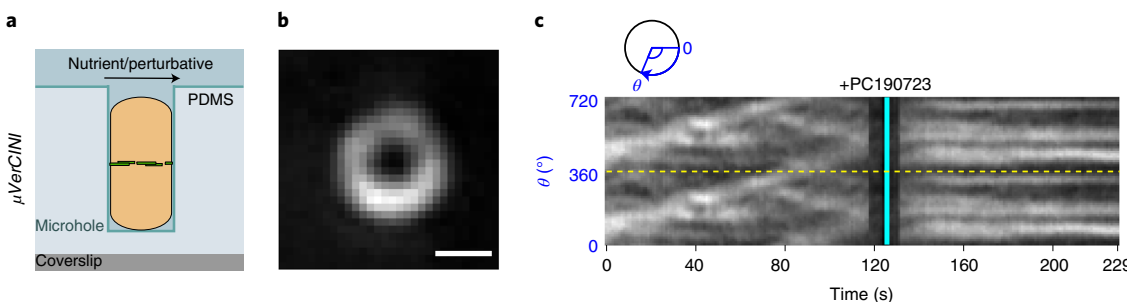


Fig. 3 | Concept of μVerCINI and demonstration of imaging division protein dynamics during rapid antibiotic perturbation. **a**, Schematic depicting a cell confined vertically in an open-topped PDMS microhole inside a microfluidic chamber, with its division ring (green dashed lines) parallel to the microscope coverslip. **b**, Representative image of a *B. subtilis* cell expressing FtsZ-GFP as a sole copy of FtsZ from the native locus (strain SH130¹²). The division ring appears as a circle. Scale bar, 500 nm. **c**, Kymograph of FtsZ-GFP treadmilling dynamics from the cell in **b** around the cell circumference, during perturbation with the FtsZ-specific inhibitor PC190723 (cyan line). Two full revolutions around the cell (0–720°) are plotted side-by-side to resolve filament trajectories that cross 0°/360°, separated by a yellow dotted line. Diagonal lines pretreatment show directional motion around the full circumference of the cell, while horizontal lines post-treatment show static clusters. Raw data from ref. ¹².

The key principle behind VerCINI is to rotate the short axes of bacteria into the microscope image plane by trapping cells in narrow microholes formed from either agarose or polydimethylsiloxane (PDMS) (Figs. 1a, 2a and 3a). To trap cells vertically, a silicon micropillar array serving as a negative master of the microholes must be fabricated at sufficient resolution for precise and reproducible cell trapping. In standard VerCINI, this micropillar array is used as a mold to form a microhole array in agarose. Bacteria are then immobilized within the traps, imaged using a high-resolution inverted microscope and data analyzed using custom image processing software tailored to maximize the signal-to-noise ratio (SNR) of VerCINI microscopy data. μVerCINI uses the same principle as standard VerCINI, but additionally enables rapid drug treatment of trapped cells by immobilizing bacteria in open-topped PDMS cell traps. VerCINI can also be easily combined with denoising, super-resolution microscopy or single-particle tracking methods to further improve image quality or resolution.

Advantages and limitations

VerCINI and μVerCINI offer several benefits for imaging the short axes of cells compared with conventional imaging of horizontally oriented cells:

- **High resolution.** A slice of the short axes of the cell (e.g., the cell septum) can be viewed at high 250 nm resolution (Fig. 1, bottom), rather than either low 550 nm resolution imaging via 3D fluorescence microscopy or a thin volume of the bottom of the cell at 250 nm resolution via total internal reflection fluorescence (TIRF) microscopy (Fig. 1, top)

- *Simultaneous imaging of an entire slice of the cell short-axes plane.* An entire slice of the plane with the short axes of the cell can be imaged at once. Proteins that are primarily moving circumferentially, e.g., divisome or elongosome proteins, can then be tracked for extended periods¹², unlike TIRF, which truncates protein trajectories owing to its small illumination volume
- *High-SNR imaging of the cell poles.* By rotating cells vertically, the cell pole is placed in contact with/near to the microscope coverslip, and is also oriented to the microscope image plane. This allows high-SNR imaging of the cell poles via TIRF illumination, while at the same time improving spatial resolution. In Fig. 2, we demonstrate proof-of-concept application of VerCINI to imaging of cell pole protein dynamics

Limitations to VerCINI and μ VerCINI include the following:

- *Incompatible with long or chained cells.* Cells that are filamentous or form long unseparated chains are not likely to fit in the holes. In some cases, these issues can be rectified with appropriate genetic modifications: for example, we have found that deleting the *hag* gene (encoding flagellin) or *slrR* gene (encoding a transcriptional regulator¹⁴) in the *B. subtilis* PY79 background greatly reduces the presence of long unseparated chains of cells, enabling efficient loading into holes¹²
- *Difficult to use with cells lacking cylindrical symmetry.* Although curved cells such as *Caulobacter crescentus* can be loaded into the microholes, data analysis for such cells can be complicated by the fact that the long (curved) axis of the cell is not parallel to the (straight) axis of the microscope, except at the cell mid-plane. One possibility to rectify this may be to first straighten such cells by deleting genes giving them curvature (e.g., *creS* in *C. crescentus*)
- *μ VerCINI requires some nonstandard microscope parts.* Due to the layer of PDMS between the microscope coverslip and vertically trapped cells, imaging with this method currently requires a special objective lens and nonstandard autofocus system. The specific reasons for this limitation and possible solutions are discussed in further detail in ‘Experimental design’

Applications

A key application for VerCINI is imaging the circumferential dynamics of cell division proteins. The septal peptidoglycan synthesis machinery moves circumferentially around the cell to build the cell wall, guided by the essential cytoskeletal protein FtsZ^{5,12}. With conventional imaging, the division plane is orthogonal to the microscope imaging plane (Fig. 1a, top), and hence the dynamics of division proteins are difficult to observe due to the background signal from out-of-focus light coming from the rest of the division ring. This background signal can be largely removed using TIRF illumination, which produces an evanescent wave that excites only the bottom 100–200 nm of the cell, but this limits imaging to only a small slice of the division septum (Fig. 1b,c, top). In contrast, VerCINI allows simultaneous imaging of the entire septum, and strongly reduces background signal, because the septum no longer overlaps itself axially.

Using an early prototype of VerCINI, we observed the circumferential dynamics of FtsZ of the model rod-shaped *B. subtilis* around the full division ring at high resolution and discovered that FtsZ filaments treadmill in the living cell (Fig. 1b,c, bottom)⁵. VerCINI has since found a variety of applications in cell division microscopy. Using an optimized version of VerCINI with increased SNR, we were able to image FtsZ dynamics at near-single-filament resolution throughout the *B. subtilis* division cycle, demonstrating that FtsZ filament condensation into a dense Z-ring drives a transition in FtsZ dynamics from a mixed population of mobile and immobile filaments to stable treadmilling during constriction initiation and active septum building. With μ VerCINI, we were also able to demonstrate that the FtsZ-targeting antibiotic PC190723 totally arrests FtsZ filament motion within seconds (Fig. 3b,c). Beyond this, VerCINI has been applied to image division in several different bacterial species using a variety of imaging methods: the dynamics of FtsZ treadmilling in the ovococcoid bacterial pathogen *S. pneumoniae*¹³, the organization of FtsZ and FtsN in *E. coli* using stimulated emission depletion (STED) super-resolution imaging¹⁵, the division-associated cell wall synthase FtsI in *E. coli* using single-particle tracking¹⁶, and peptidoglycan synthesis during division and elongation in *S. pneumoniae* using direct stochastic optical reconstruction microscopy (dSTORM) with fluorescently labeled ‘clickable’ D-amino acids¹⁷.

VerCINI also has multiple applications to cellular systems beyond cell division. Since the cell wall is synthesized circumferentially in many bacteria, nearly any protein involved in these processes is an ideal candidate for investigation with VerCINI. For example, we are currently using single-particle tracking to image the circumferential motion of the elongation-associated cytoskeletal protein MreB in *B. subtilis* (unpublished). Another possible application of VerCINI is the bacterial nucleoid and

associated proteins, which may show substantial radial organization due to the combined effects of transcription and translation¹⁸. The general concept of using vertical cell immobilization to improve imaging resolution has also been applied successfully to eukaryotic systems, although both the microfabrication and microscopy approaches required differ substantially due to the much larger cell size^{19–21}.

We believe that a major potential application of VerCINI is the imaging of cell poles. Vertical orientation increases the spatial resolution of cell pole organization, and high-SNR imaging with TIRF illumination becomes uniquely possible as the cell pole is placed in contact with the microscope coverslip. To illustrate this, we provide brief proof-of-concept demonstration of VerCINI to cell pole imaging by investigating the dynamics of the *B. subtilis* chemoreceptor protein TlpA (Fig. 2; Supplementary Methods). TlpA is a chemoreceptor protein in *B. subtilis* that forms large clusters localized to both the base of division septa and cell poles (Fig. 2a,b), likely due to a binding preference for regions of high membrane curvature²². With conventional imaging, the distribution and dynamics of these clusters are obscured by the signal from overlapping clusters (Fig. 2b, top). In contrast, orienting cells vertically with VerCINI and illuminating via TIRF allows for high-resolution and high-SNR imaging of these clusters at cell poles (Fig. 2b–d). We observed that TlpA forms multiple large, essentially immobile clusters (generalized diffusion coefficient $\langle K_a \rangle = 5 \cdot 10^{-7} \pm 6 \cdot 10^{-7} \mu\text{m}^2/\text{s}$ (mean \pm standard deviation (SD)) for the data shown in Fig. 2) of varying size, consistent with large chemoreceptor arrays observed in other organisms by cryo-electron tomography²³ (Fig. 2b–d, bottom).

This protocol was optimized using *B. subtilis* strain PY79, although it is applicable to a wide range of bacterial cell types. We have used it to image *B. subtilis* 168, *S. pneumoniae* D39¹³, *Corynebacterium glutamicum* RES 167 and *E. coli* MG1655, while others have used it to image *S. pneumoniae* strain R800¹⁷. This protocol should be generally applicable to any bacterial cell type with cylindrical symmetry. Preliminary VerCINI measurements of the curved, noncylindrical *Caulobacter crescentus* also gave successfully trapped cells, indicating that VerCINI may be also applicable to other curved rod-like cells.

Experimental design

Nanofabrication of micropillars

We use e-beam lithography and deep reactive ion etching to create the micropillars on a silicon wafer using an approach similar to that of Deshpande and Dekker²⁴.

We designed square microholes, as we hypothesized that a deformable material like agarose should trap cells more efficiently than circular ones owing to a small number of cell–microhole contact points, leading to a larger fit tolerance. The following protocol is therefore for an array-of-squares pillar pattern (Fig. 4c). Software for each step of the nanofabrication protocol is publicly available in a package called VerCINI_nanofab on GitHub²⁵.

Since each silicon wafer can easily be split into four quarters, we recommend making four identical patterns—one in each quadrant (Fig. 4c)—to maximize the utility of the wafer. Although space is available on the wafer to accommodate larger arrays, we use an overall pattern size of $\sim 1 \times 0.5 \text{ cm}^2$ because the agarose pad that will eventually contain this pattern will need to be cut down prior to imaging to ensure sufficient oxygen delivery to trapped cells.

When using VerCINI for the first time, we recommend making several columns of differently sized pillars (Fig. 4c) to later find the optimal size for your particular bacteria and growth conditions (for *B. subtilis* we have found that pillars of width 1.0–1.3 μm work best). Importantly, we have found that the Bosch etching process shrinks the squares substantially (Fig. 5a,b) from the designed widths owing to some degree of ‘isotropic etching’ (i.e., undercutting the resist), and so the designed widths must be larger to compensate. The amount that pillars shrink during the Bosch etch depends on both the sizes of gaps between pillars (Fig. 5c) and the duration of the Bosch etch. For gaps of 3.0–3.5 μm , we have measured a decrease in widths of $560 \pm 110 \text{ nm}$ (mean \pm SD) for a 100 s Bosch etch ($N = 204$ pillars from $N = 4$ wafers) and $680 \pm 40 \text{ nm}$ (mean \pm SD) for a 140 s Bosch etch ($N = 76$ pillars from $N = 2$ wafers). However, for a given gap size and Bosch etch time, we have found that the decrease in pillar widths is reproducible.

One other critical factor when designing the array-of-squares pattern is e-beam write time. Since it takes much more time for the e-beam system to move the sample stage than to deflect the beam, moving the stage to write each individual square shape will require a prohibitively long amount of time. However, the area over which the e-beam can write at a single stage position (the main field; $\sim 1 \times 10^6 \mu\text{m}^2$ for our Raith

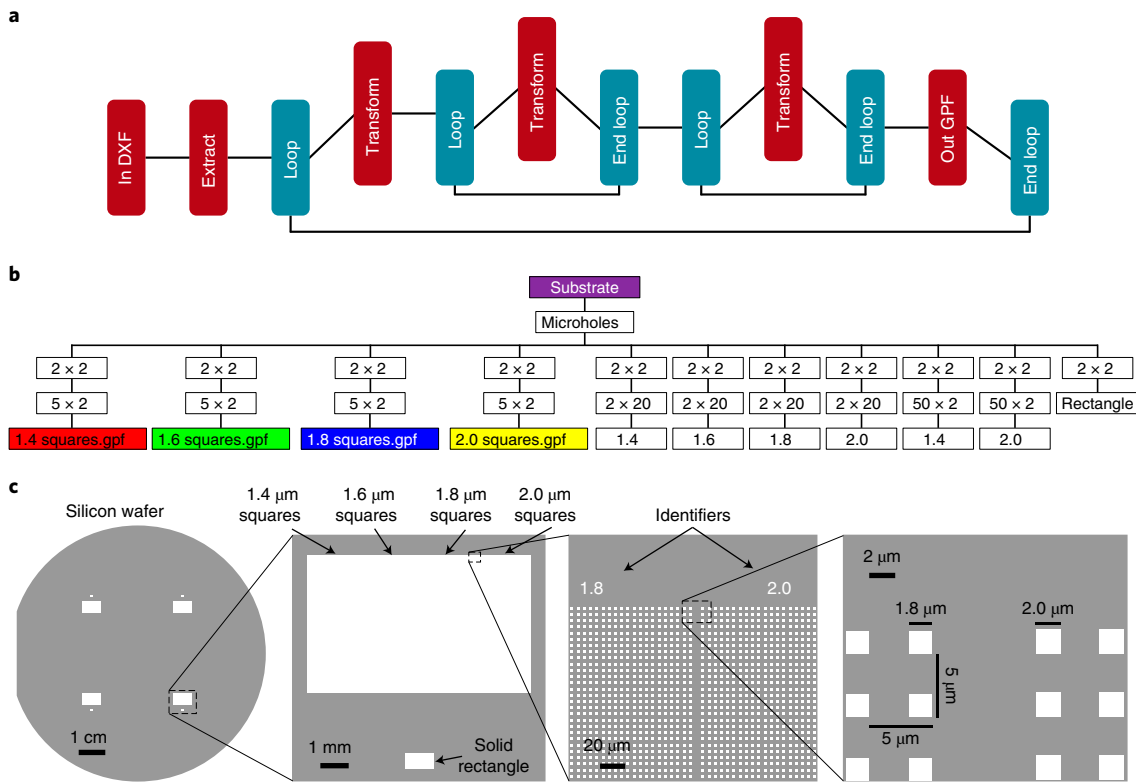


Fig. 4 | Design of micropillar wafer. **a**, Algorithm of LayoutBEAMER used to produce arrays of squares the size of the e-beam machine's main field. **b**, Algorithm of Cjob used to produce full arrays of squares of four different sizes in each quadrant of a wafer, along with identifiers and solid rectangle for measuring height after etching. **c**, Output of Cjob code and overall design of silicon wafer showing arrays of squares of four different sizes in each quadrant of the wafer, along with identifiers and solid rectangle.

EBPG-5000+) is much larger than each individual square that will be written ($\sim 1 \mu\text{m}^2$). So, the protocol below describes how to produce an array of squares that is roughly the same size as the e-beam's main field, and then later replicate this array to obtain a larger array pattern. This way, thousands of squares are written at each stage position, dramatically reducing the e-beam write time.

One further consideration is the heights of pillars that will be needed. The optimal heights are mainly determined by the average length of cells that users want to eventually image in microholes (for *B. subtilis* we typically use pillars of height 4–7 μm). Pillars can also be made taller to accommodate longer cells or multiple short cells as a column, but taller (i.e., higher aspect ratio) pillars are more fragile and susceptible to breaking when agarose or PDMS are peeled off them. We have successfully used pillars with aspect ratio up to ~10 (1 μm square pillars 10 μm tall), but it is likely that pillars with much higher aspect ratios will not be feasible. To further prevent pillars breaking when PDMS is peeled off, we coat the wafers with a silane compound (tridecafluoro-1,1,2,2-tetrahydrooctyl trichlorosilane) by vapor deposition to prevent strong adhesion. Although designed to enable solidified PDMS to be removed, we also found that this silane coat makes solidified agarose peel off more easily as well.

For researchers that do not have access to a nanofabrication facility, silicon wafers for VerCINI can be fabricated commercially on the basis of this protocol. We are currently performing prototyping and testing with ConScience AB, Sweden, to make VerCINI chips available to other researchers, without financial benefit to ourselves. ConScience have an estimated production cost of \$2,900 per wafer (\$700 per VerCINI chip). The authors or the company may be contacted for updates. Other companies should also be able to fabricate these devices.

Sample preparation and imaging

To image cells during vegetative growth, VerCINI pads are made using agarose dissolved in growth media using an approach adapted from de Jong et al.²⁶. The porous nature of the agarose gel allows nutrients to diffuse through to cells, allowing continued growth during the imaging process, while a high agarose concentration makes the gel stiff, providing structural stability to the microholes.

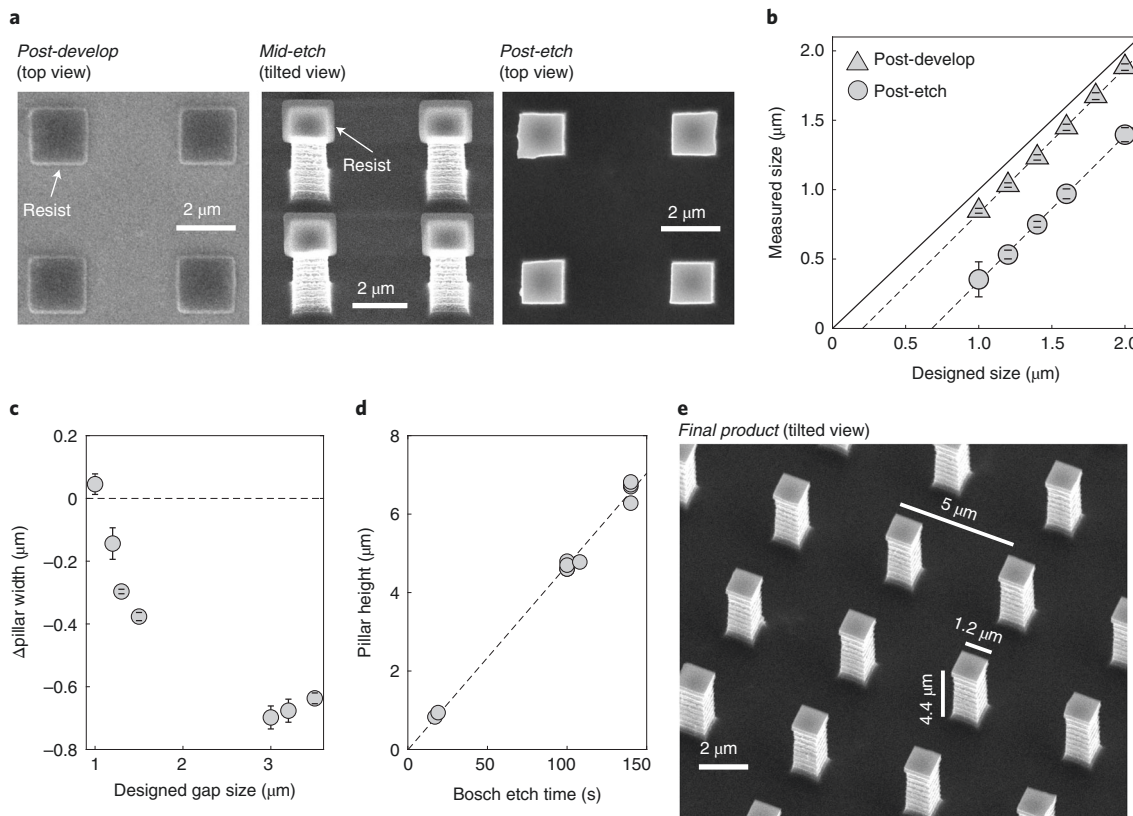


Fig. 5 | Development and etching of micropillar wafer. **a**, SEM image of silicon wafer with squares with designed edge lengths of 2.0 μm during development and etching. Left: patterned squares of e-beam resist remaining after development, seen from top down. Middle: patterned squares after several cycles of Bosch etch, but before removing resist with oxygen plasma, seen from a tilted angle. Etching produces substantial undercutting. Right: patterned squares after etching and oxygen plasma to remove resist, seen from top down. Scale bar, 2 μm. **b**, Comparison of designed square sizes to measured square sizes after development (triangles) and after 100 s of Bosch etch (circles) for a pattern with 5 μm spacing. Solid line shows hypothetical 1:1 correlation. Dotted lines show linear fits to post-develop and post-etch data. Post-develop: $N = 209$ squares; post-etch: $N = 66$ pillars. Error bars are SD. **c**, Change in widths of pillars after 140 s Bosch etch compared with designed size of gaps between pillars. Results from $N = 123$ pillars from four wafers. Error bars are SD. **d**, Effect of etch duration on final heights of micropillars. Each circle represents a separate wafer or wafer quarter ($N = 11$ wafers total). Wafers had different square sizes, but all had spacing of 5 μm. Dotted line: linear fit to data. **e**, SEM image of a final silicon micropillar wafer with measured widths ~1.2 μm and spacing 5 μm (and, hence, gap of 3.8 μm between pillars). Heights were measured to be 4.4 μm from profilometer.

One critical factor for VerCINI is the efficiency with which cells are loaded into holes. A higher loading efficiency corresponds to more trapped cells in a single field of view (FoV), and therefore greater data acquisition. We have found that centrifuging concentrated cell culture into the holes using a flat-bottomed centrifuge rotor gives high loading efficiency (Fig. 6c,d).

Another important consideration is that cells are sometimes poorly trapped in the holes, causing them to wobble (Supplementary Video 1). Although these are relatively rare for correctly sized micropillars, imperfectly trapped cells can be identified and removed from further analysis by recording a short (~1 s) bright-field video after fluorescence acquisition. We initially hypothesized that flagellar motility might cause this poor trapping. However, at least in *B. subtilis*, this does not appear to be the case, as deleting the *hag* gene made little difference to the amount of poorly trapped cells. In the less chain-forming *B. subtilis* strain BS168, we frequently perform experiments in motility-proficient cells without issue.

After loading, cells can be imaged using any microscope technique suitable for studying bacterial spatial organization. Importantly, microholes are imprinted on the top of the agarose pad, so the cells are adjacent to the coverslip surface (Figs. 1b and 2b). This means that illumination techniques such as highly inclined and laminated optical sheet (HILO) (for cell sidewall; e.g., Fig. 1b) and TIRF (for cell poles; e.g., Fig. 2b) are preferable to maximize image SNR. We employ a ring-TIRF or ring-HILO system, where galvanometer-driven mirrors rotate the illumination beam at high speed (200 Hz) to produce uniform illumination across the sample²⁷; however, single-angle TIRF or HILO is also sufficient.

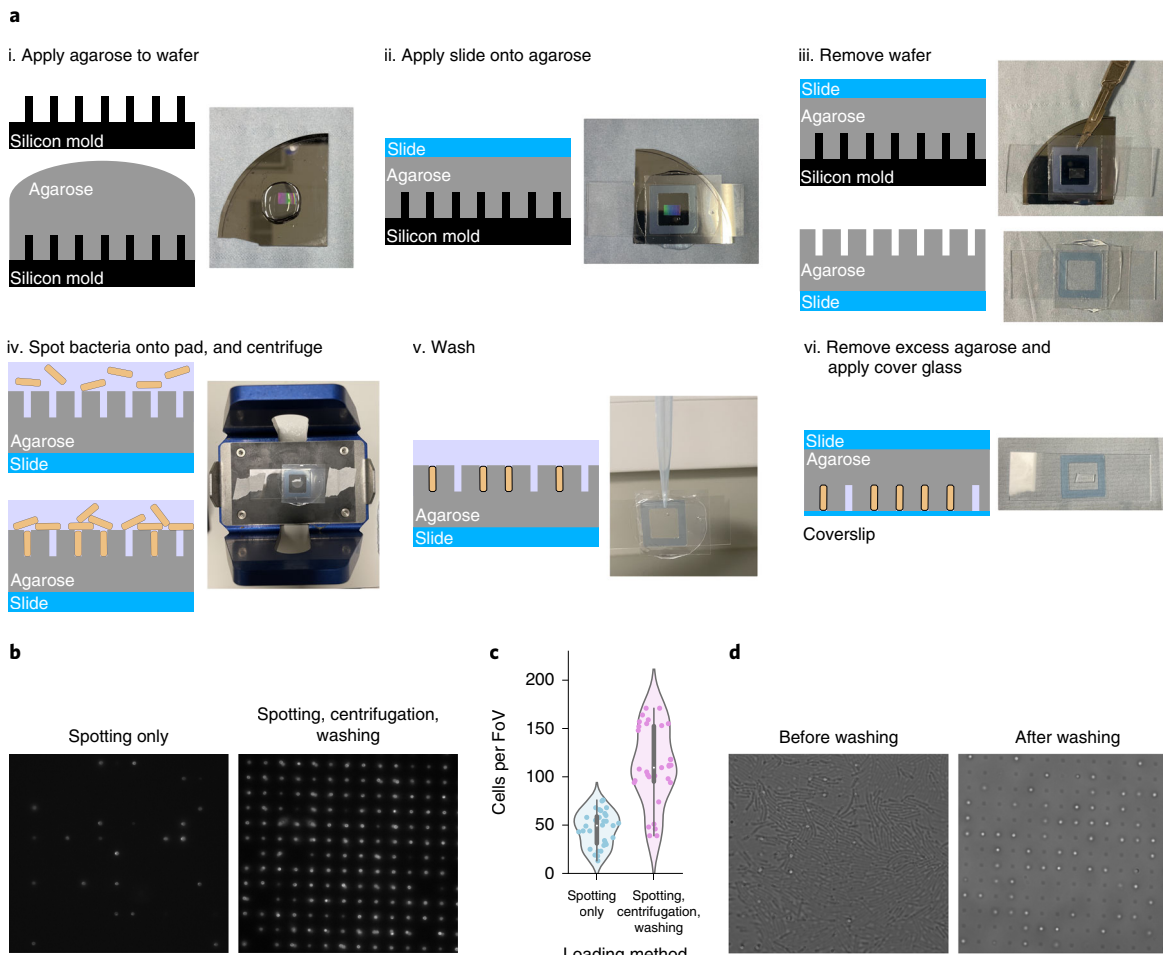


Fig. 6 | Sample preparation for VerCINI. **a**, Sample preparation workflow. (i) Molten agarose is applied to the silicon micropillar wafer; (ii) the cover slide is applied onto the agarose with Gene Frame down; (iii) the micropillar wafer is removed from the agarose slide; (iv) concentrated bacteria are pipetted onto the imprinted agarose, and the slide is centrifuged to increase loading efficiency; (v) excess horizontal cells are washed off the pad; (vi) excess agarose is cut away from the pad, leaving only the microhole imprinted area, and the cover glass is applied. **b**, HILO VerCINI of *B. subtilis* cells expressing FtsZ-GFP (strain SH130¹²) loaded into microholes with or without centrifugation. Left: cells loaded only by spotting liquid culture onto the VerCINI pad and applying the coverslip. Right: cells loaded by spotting concentrated liquid culture, centrifuging and washing off unloaded cells. **c**, Violin plots comparing loading efficiency between the two loading methods shown in **b**. White circles, median; thick gray lines, interquartile range; thin gray lines, 1.5× interquartile range. Spotting only: $N = 31$ FoVs from six independent experiments; spotting, centrifugation, washing: $N = 31$ FoVs from three independent experiments. **d**, Bright-field images of SH130, before and after the washing step.

μVerCINI

In many experiments, researchers want to perform rapid solution exchange during imaging, either to change from one medium to another, to add perturbatives such as antibiotics, to fix cells or to label cells with exogenous dyes. However, with the original VerCINI method this is not possible since the slide is closed and the cells are underneath a dense pad of agarose. We have therefore designed an adapted version of the method to be compatible with solution exchange, μVerCINI. In this method, the microholes are open-topped (Fig. 3a), and the cells are exposed to a fluid environment that is controlled by users through a microfluidic system.

One critical difference with this open-topped orientation is that there is a layer of material between the coverslip surface and the cells through which imaging will be done. Making a thin layer with agarose is challenging, and imaging through a thick layer of agarose would lead to substantial loss in image quality due to scattering. We instead use PDMS, which forms a relatively thin (~50 µm) transparent layer (Fig. 7a).

Because the holes are formed of PDMS rather than agarose, loading cells into the holes of a μVerCINI coverslip differs somewhat from VerCINI. PDMS is normally quite hydrophobic, and the surface tension of an aqueous cell culture is high enough that the microholes will end up filled with

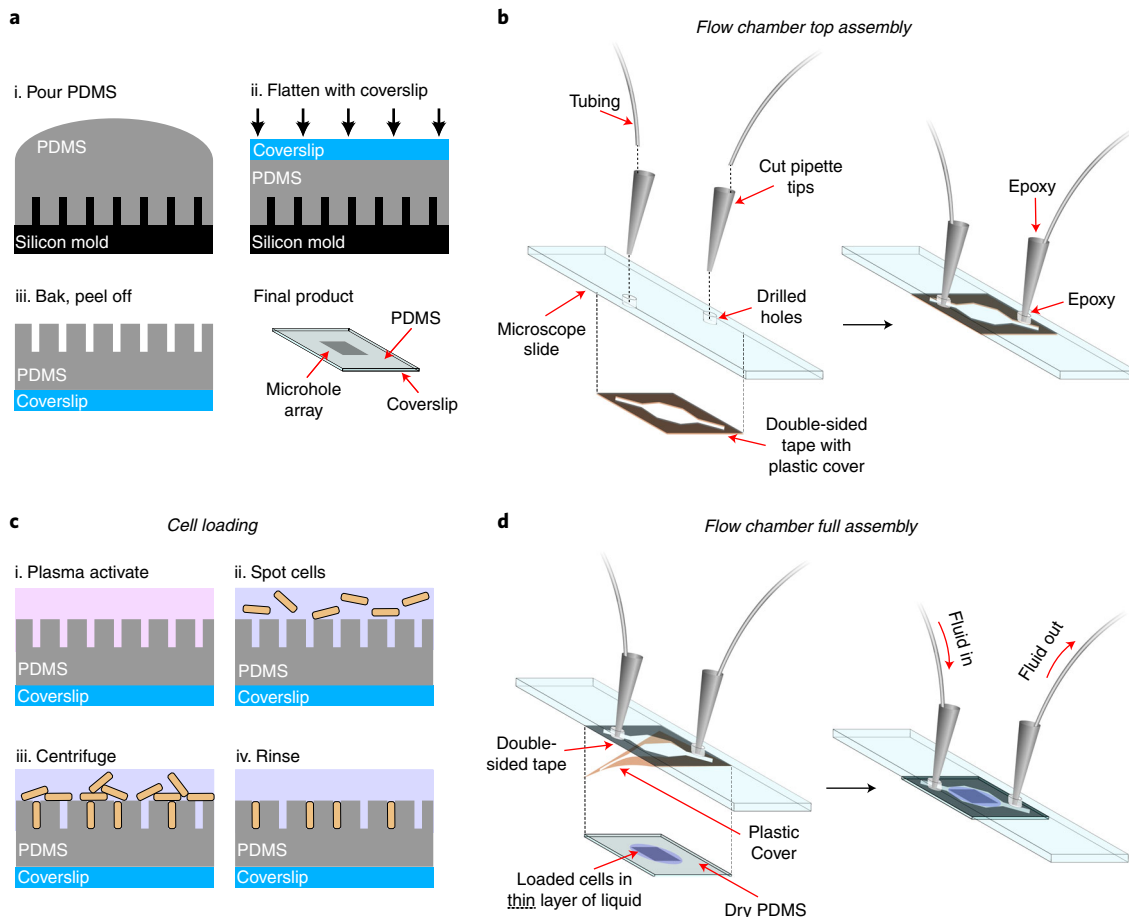


Fig. 7 | Device assembly and cell loading for μ VerCINI. **a**, Assembly of μ VerCINI coverslip. (i) Degassed PDMS in a 10:1 elastomer base: curing agent ratio is poured onto silicon micropillars; (ii) a coverslip is pressed firmly down on top of the PDMS to form as thin a layer as possible; (iii) the PDMS is baked in an oven and peeled off to produce a coverslip with open-topped PDMS microholes. The final product can be stored for months to years. **b**, Assembly of top of flow chamber. A microscope slide has holes drilled into it. Cut pipette tips are inserted into these holes and epoxied in place, and tubing is inserted into the cut pipette tips and epoxied in place. A piece of double-sided tape with plastic cover still attached has a groove cut into it and is adhered to the microscope slide. The final product can be stored for months to years. **c**, Loading cells into open-topped microholes. (i) PDMS is rendered hydrophilic through treatment with air or oxygen plasma; (ii) cell culture is concentrated and added on top of the microholes; (iii) the μ VerCINI coverslip with concentrated cell cultures is centrifuged to load cells into holes; (iv) cells not loaded into holes are rinsed off with fresh medium. **d**, Assembly of full flow chamber with loaded cells. The PDMS μ VerCINI coverslip is dried around the edges, and all but a thin layer of liquid is left above the loaded cells. The plastic cover of the double-sided tape is removed, and the tape is adhered to the PDMS. The final product is a closed chamber through which fluid can be flowed.

air bubbles rather than liquid or cells. PDMS is therefore first rendered hydrophilic by treatment with oxygen or air plasma (Fig. 7ci).

After cells are loaded, the μ VerCINI coverslip is adhered to a prefabricated device (Fig. 7b) to form a closed microfluidic chamber (Fig. 7d). This device consists of a microscope slide with drilled holes to allow for inlet and outlet tubing, along with a piece of double-sided tape that has been cut to form a flow channel. The double-sided tape serves two functions: it forms a thin (~100 μ m) flow channel between the microscope slide and the tops of the microholes, and it seals the whole system together. It is important to identify a suitable double-sided tape as not all brands of double-sided tape adhere well to PDMS, which can produce leaks. We have found that Duck and Club brand double-sided tapes work well, while Scotch, Sellotape and WHSmith double-sided tapes do not.

There are two key points to consider when imaging with μ VerCINI. First, even with a relatively thin 50 μ m PDMS layer on top of a #1.5 microscope coverslip, we found that we cannot successfully acquire images using a high-numerical-aperture oil immersion 100 \times TIRF objective. This is likely due to spherical aberration resulting from refractive index mismatch between PDMS ($n = 1.43$) and glass ($n = 1.52$). We instead use a silicone immersion oil objective since the silicone oil refractive index

($n = 1.41$) is similar to PDMS. This objective also has a large working distance (0.3 mm), which is useful for imaging through the PDMS layer.

Second, μ VerCINI is not compatible with reflection-based autofocus systems. This is because very little reflection occurs off the PDMS/liquid interface, as the indices of refraction are too similar (~1.43 and ~1.33, respectively). One possible solution is to use image-based autofocus methods (e.g., Micro-Manager's OughtaFocus); however these are not suitable for correcting drift during high-speed imaging of protein dynamics. A solution that we favor is to use an image-based autofocus system that measures drift using the cross-correlation between images and a reference stack in a separate infrared (IR) bright-field illumination and imaging pathway²⁸. We developed a custom plugin for Micro-Manager to set the reference stack, calculate the cross-correlation maps and maintain sample focus by closed-loop positioning of the microscope stage¹². We perform the IR drift correction method on a custom built high-resolution microscope, but the apparatus for this method can also be retrofitted onto commercial microscopes²⁸. If automated drift correction methods are not available, with practice it is possible for a skilled operator to continuously manually correct for drift during image acquisition. However, this will usually lead to reduced image quality due to increased periods of defocus during data acquisition.

It is also important to note that, unlike VerCINI, μ VerCINI is often used for ‘single-shot’ experiments, which limits users to recording a single FoV. For example, if a researcher wants to image the effect of an antibiotic perturbation on protein dynamics inside cells (e.g., Fig. 3c), then the experiment cannot be repeated on a different FoV with the same slide, as all cells on the slide have already been perturbed. Because of this it is imperative not only to have high loading efficiency, but also to take some time to scan across the slide and find the best possible FoV before beginning.

Image processing and analysis

We focus here on our most common case of VerCINI image analysis: analysis of protein motion around the cell circumference or cell septum via kymograph analysis. This analysis method is appropriate when protein motion is mostly restricted to the leading edge of the cell septum (e.g., FtsZ) or the cell sidewall (e.g., MreB or other elongosome proteins). For other datasets, such as TIRF imaging of cell-pole-localized proteins, other analysis methods such as single-molecule tracking may be more appropriate. The overall workflow for image processing and analysis is shown in Fig. 8a.

The first steps of image processing are done in Fiji/ImageJ²⁹. We have developed a plugin called VerciniAnalysisJ specifically for processing VerCINI videos, which can be installed from the VerciniAnalysisJ update site with all its dependencies. Later image processing steps such as subtracting the cytoplasmic background signal and producing kymographs are done in MATLAB. We have developed software for these steps in a package called ring-fitting2 that is publicly available on GitHub³⁰.

Two key processing steps are image denoising and registration. We found that image denoising allows us to substantially reduce illumination intensity while still maintaining high SNR, thereby minimizing photobleaching and phototoxicity. We strongly recommend denoising VerCINI data prior to subsequent analysis. While a number of denoising algorithms have been developed, we use the ImageJ plugin PureDenoise, which is based on wavelet decomposition³¹. One advantage to using this algorithm is that it does not make any assumptions about the underlying biological structure. After denoising, any global image drift—for example, due to agarose contraction—is corrected via image registration using the ImageJ plugin StackReg³².

Our ring-fitting2 software automatically extracts kymographs of circumferentially localized protein dynamics¹² (Fig. 8d,e). This software also subtracts the diffuse out-of-focus cytoplasmic background (Fig. 8d), which can otherwise obscure protein dynamics. The background signal is subtracted from the image stack for each frame, and then the intensity around the fitted circle is calculated to subpixel precision via interpolation. We found that subpixel fitting of the cell center and septum/circumference and robust background subtraction were crucial to obtaining accurate intensity measurements. During software development, we observed that small inaccuracies in cell center localization, caused for example by fitting an annulus with uniform instead of sectored amplitude, would cause large errors in apparent septal intensity as the small size of the cell, together with the complex background, meant that different amounts of background signal would be integrated on either side of the cell. To confirm that the microscope system and image processing pipeline are together giving even circular symmetric intensity measurements around the center of the cell, a cell expressing cytoplasmic GFP can be imaged and analyzed. An example script for this purpose is supplied in the VerCINI analysis software.

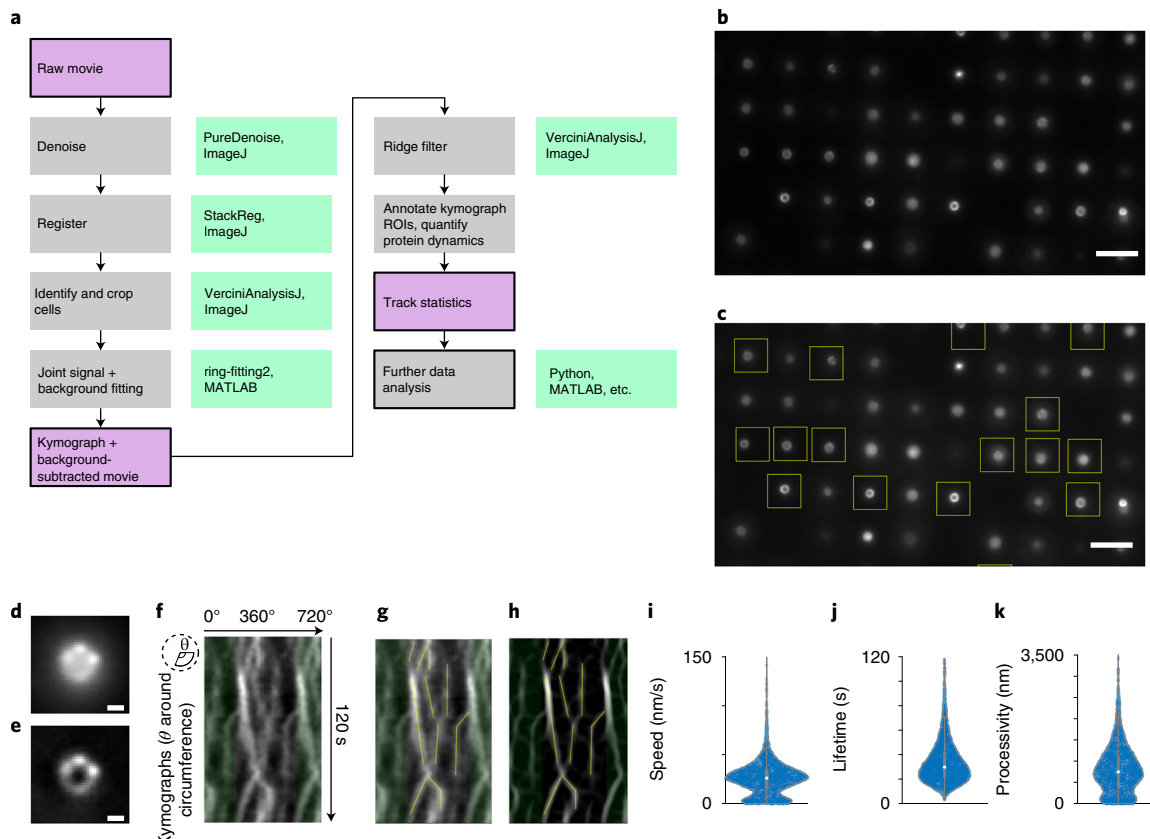


Fig. 8 | Image processing and analysis for VerCINI and μ VerCINI. **a**, VerCINI image processing workflow diagram. Purple box, data. Gray box, Image/data processing step. Green box, software tool to perform image/data processing step. **b**, Exemplar VerCINI image of *B. subtilis* cells expressing FtsZ-GFP. Scale bar, 5 μ m. **c**, ROIs around in-focus cell septa/circumference are manually identified and cropped for further analysis. Scale bar, 5 μ m. **d**, Exemplar denoised VerCINI image of a single cell. Scale bar, 0.5 μ m. **e**, Background-subtracted image using joint model-based VerCINI fitting and background-subtraction algorithm. **f**, Kymograph around septum of background-subtracted cell in **e**. **g,h**, Annotated raw kymograph (**g**) and ridge-filtered kymograph (**h**). Line ROIs indicate manually detected and annotated filament trajectories. Green regions in **f-h** indicate a repeated section of the kymograph added to visualize filament trajectories crossing the boundary of the circular profile. **i-k**, Exemplar violin plots of FtsZ-GFP filament dynamics measured by VerCINI. White circles, median; thick gray lines, interquartile range; thin gray lines, 1.5 \times interquartile range. Raw data in **b-k** from ref. ¹².

Processive protein motion is visible on kymographs as a diagonal line, with line angle indicating protein speed. For dense protein filaments such as FtsZ, we currently quantify protein speed, bound lifetime and other parameters such as directional switching and pausing by manual kymograph annotation (Fig. 8g,h), as we found that most automated kymograph annotation methods do not perform well at high density. An ImageJ macro is provided for quantification of filament dynamics via manual ImageJ regions of interest (ROIs) annotation. During kymograph analysis, it can be difficult to identify trajectories of dim filaments owing to the large intensity range within kymographs. This issue is frequently encountered for analysis of FtsZ dynamics in dense Z-rings. To address this issue, we recommend applying a ridge detection filter to the kymograph, which detects peaks within an image irrespective of intensity based on the image second derivative. A script ‘Ridge_Filter.ijm’ is provided for this purpose. We note that a recent deep-learning-based kymograph annotation tool could enable automated processing of VerCINI kymographs in the future³³.

Level of expertise needed to implement the protocol

The nanofabrication protocol we describe to obtain a micropillar silicon wafer requires a cleanroom facility with appropriate training. This requirement can be avoided by ordering commercially fabricated wafers. Once a micropillar wafer is available, the rest of the VerCINI/ μ VerCINI protocol can be performed in any bacteriology laboratory with expertise in live single-cell resolution fluorescence microscopy. Although μ VerCINI does not require prior expertise in soft lithography or microfluidics, it is more difficult than VerCINI owing to some specialized hardware and more complicated

assembly. We therefore recommend users to become experienced at using VerCINI (Part 1) prior to trying μ VerCINI (Part 2).

Materials

Reagents

- Silicon wafer (4 inch diameter, 500 μm thickness, one side polished, type/orientation NP<100>, PB<100>, resistivity 1–10 $\Omega\text{ cm}$; International Wafer Service)
- 1,1,1,3,3,3-hexamethyldisilazane (HMDS; VWR, cat. no. 51152885) **! CAUTION** This compound is highly flammable and is toxic on contact with skin or if inhaled. Wear protective gloves, protective clothing, eye protection and face protection.
- Negative e-beam resist (e.g., AR-N-7700.18; Allresist)
- Developer (e.g., Microposit MF-321; micro resist technology)
- (Tridecafluoro-1,1,2,2-tetrahydrooctyl)trichlorosilane (abcr, cat. no. AB111444) **! CAUTION** This compound is flammable, and causes severe skin burns and eye damage. It reacts with water to produce hydrogen chloride. Wear protective gloves, protective clothing, eye protection and face protection. Work in a dry, inert gas atmosphere while handling. Once aliquoted, flush the stock bottle with argon and seal the lid with parafilm.
- Ultrapure agarose (Invitrogen, cat. no. 16500–100)
- PDMS elastomer base (Dow Corning, Sylgard 184 elastomer base)
- PDMS curing agent (Dow Corning, Sylgard 184 elastomer curing agent)
- Cell growth medium (experiment-specific, but ideally should have low autofluorescence)

Biological materials

- Bacterial cell type of interest. This protocol should be generally applicable to any bacterial cell type with cylindrical symmetry, although it may also apply to noncylindrical cells. The cell types we used to optimize the procedure and generate the data in this protocol (available upon request to the authors) are:
 - *B. subtilis* SH130 (PY79 Δ hag *ftsZ*::*ftsZ*-*gfp*-*cam*)¹²
 - *B. subtilis* HS48 (168 *amyE*::*spc* P_{xyl} -*tlpA*-*mgfp*)²²

Equipment

Cleanroom equipment

- Spin-coating system (SUSS MicroTec)
- Hot plates (Harry Gestigkeit, cat. no. 2860EB)
- Syringe, 5 mL (e.g., BD Plastipak, cat. no. 309649)
- Syringe filter, 0.22 μm (e.g., Starlab, cat. no. E4780-1221)
- Electron-beam lithography system (Raith, model no. EBPG5000+)
- Upright microscope (Olympus, model no. BX51M)
- Deep reactive ion etching system (Adixen; AMS, model no. 100 I-speeder)
- Stylus profilometer (Bruker, model DektakXT)
- Scanning electron microscope (SEM; e.g., FEI, NovaNano SEM)

Wet lab equipment

- Inert gas (e.g., argon) supply
- Vacuum desiccator (Kartell)
- Vacuum pump (Leybold Trivac, model no. D8B)
- Diamond scribe (e.g., RS Pro, stock no. 394–217)
- Gene Frames, 65 μL , 1.5 \times 1.6 cm^2 (Thermo Scientific, product code 11560294)
- Microwave
- Water bath with heater (e.g., Grant, model JB Nova)
- Mini-centrifuge (Eppendorf, model 5424)
- Silicone gaskets (Sigma-Aldrich, cat no. GBL103240), cut into individual 9 mm gaskets
- Centrifuge (VWR, model 5810, cat. no. EPPE5810000.060)
- Rotor with flat-bottomed buckets (VWR, A-4-81 Swing-out Rotor with 4 \times MTP/Flex Buckets, cat. no. 521-0145)
- Oven (e.g., Falc Instruments, Mini Oven STZ 5.4)
- Flat blade (e.g., Stanley 18 mm snap off blades, cat. no. 0-11-301)

- Power drill (e.g., Dremel, Dremel 4000)
- Multi-chuck for power drill (e.g., Dremel, 0.8–3.2 mm keyless chuck)
- Diamond-tipped drill bits, 0.75 mm (Kingsley North, cat. no. 1-0500-100)
- Double-sided tape (e.g., Duck, 38 mm × 5 m)
- Pipette tips (e.g., Starlab, 10 µL, cat. no. S1111-3000)
- Polyethylene tubing, inner diameter 0.38 mm, outer diameter 1.09 mm (Smiths Medical, cat. no. 800/100/120)
- Rapid-drying epoxy (Araldite, Rapid 2 × 15 ml)
- Needles, 0.45 mm × 10 mm (26G × 3/8") (BD Microlance, cat. no. 300300)
- Plasma cleaner (Harrick Plasma, cat. no. PDC-002-CE)
- Syringe, 20 mL (e.g., BD Plastipak, cat. no. 301189)
- Syringe pump (Aladdin-220; World Precision Instruments)

Microscopy equipment

- Microscope slides (e.g., VWR Super Premium, cat. no. 631-0908)
- Microscope coverslips, 22 × 22 mm², thickness no. 1.5 (e.g., VWR, cat. no. 631-0125)
- Inverted fluorescence microscope, preferably with laser-based TIRF/HILO illumination (e.g., Nikon N-STORM)
- 100× oil immersion objective (e.g., Nikon, CFI Apochromat TIRF 100XC Oil)
- 100× silicone oil immersion objective (Nikon, CFI SR HP Plan Apo Lambda S 100XC Sil, for µVerCINI only)
- Microscope incubation or stage heating device (for live-cell microscopy)

Software

- Computer-aided design (CAD) software (e.g., AutoCAD (Autodesk), <https://www.autodesk.eu/products/autocad/overview>)
- BEAMER (GenISys, <https://www.genisys-gmbh.com/beamer.html>)
- Cjob (Vistec Lithography)
- Image acquisition software (e.g., Micro-Manager v2.0gamma, <https://micro-manager.org/>)
- Fiji v1.53 (<https://fiji.sc>)
- VerciniAnalysis ImageJ plugin (<https://github.com/HoldenLab/VerciniAnalysisJ>)
- MATLAB (Mathworks)
- ring-fitting2 MATLAB package (<https://github.com/HoldenLab/ring-fitting2>)

Procedure

Design of an array-of-squares pattern ● Timing ~30 min – 2 h

- 1 Make a 1 × 1 µm² square in AutoCAD. Save it as a dxf file.
- 2 In BEAMER, make an array of squares the size of the e-beam main field. One possible algorithm to achieve this is shown in Fig. 4a.
 - Input the dxf file containing the square
 - Use one loop to scale the square to a range of different sizes, as desired (e.g., 1.4–2.0 µm edge lengths)
 - Within this loop, use two more loops in series to make an array of squares in X and Y, selecting the option to merge the results of all loops rather than to only keep the final loop iteration. Arrays of each desired square size will be output as a separate gpf file

? TROUBLESHOOTING

- 3 In Cjob, load the gpf files from BEAMER and replicate them several times to make four full arrays, one in each quadrant of the wafer. Also add in identifiers and a solid rectangle to measure heights. A code structure to achieve this is shown in Fig. 4b.
 - For Substrate, choose a 100 mm diameter silicon wafer and 100 kV exposure
 - Using Layout, replicate all patterns in each quadrant of the wafer to maximize its use (2 × 2)
 - Again using Layout, replicate the gpf files from BEAMER to make a large array pattern in each wafer quadrant. We repeat the pattern twice in the X direction and five times in the Y direction. Select the following parameters for writing: dose = 117 µC/cm² (for AR-N-7700 resist), beam step size = 25 nm, beam size = 56 nm
 - Add identifiers around the entire array so that the sizes can be identified later under a microscope. Select the following parameters for writing: dose = 117 µC/cm², beam step size = 50 nm, beam size = 95 nm

- Add a solid $1,000 \times 500 \mu\text{m}^2$ rectangle above each array so that the heights can be measured with a profilometer after etching. Write the rectangle with the parameters: dose = $117 \mu\text{C}/\text{cm}^2$, beam step size = 50 nm, beam size = 95 nm
- Export the file as a job to the e-beam system

Fabrication of a silicon micropillar wafer ● Timing ~3 h

▲ CRITICAL Steps 4–10 should be performed in a cleanroom facility (for this work, a class 10,000 (International Organization for Standardization 7) facility with a class 100 (International Organization for Standardization 5) work area was used). These steps are adapted from Deshpande and Dekker²⁴.

- 4 Spin-coat the wafer with negative e-beam resist.
 - Prime a 4 inch diameter silicon wafer by spreading ~5 mL HMDS on the polished side, and spin-coating it at 1,000 rpm for 1 min. Immediately bake the wafer at 200 °C for 2 min. HMDS will increase adhesion of the resist. (Prior to spin-coating, the wafer can optionally be cleaned with fuming nitric acid to remove dust and impurities. This is recommended to prevent nonuniform deposition of resist on the wafer during spin-coating and hence ensure that the patterns avoid defects arising from this. However, we have found that this step is typically unnecessary if fresh silicon wafers are used straight from packaging.)
 - Using a 0.22 μm filter, carefully spread ~5 mL of AR-N-7700.18 resist on the wafer. If bubbles appear, gently move them away from regions where patterns will be written using either the tip of the syringe filter or a cleanroom wipe. Spin-coat the wafer at 500 rpm for 1 min, then immediately bake at 85 °C for 2 min

? TROUBLESHOOTING

- 5 Write the array-of-squares micropillar pattern on the coated wafer using an electron-beam lithography system following the manufacturer's instructions.
- 6 Bake the wafer immediately after writing at 105 °C for 2 min. **▲ CRITICAL STEP** Failure to bake the wafer will result in patterned region dissolving during development.

■ PAUSE POINT The baked wafer can be kept at room temperature (RT, ~22 °C) in a dust-free environment indefinitely.

- 7 Develop the wafer to remove the resist that was not exposed to the e-beam (Supplementary Fig. 1).
 - Soak the wafer in MF-321 for 90 s, and swirl gently
 - Immediately, soak the wafer in diluted MF-321 solution (10% (vol/vol) MF-321 in water) for 30 s, and swirl gently
 - Immediately, soak the wafer in water for at least 30 s, swirling gently
 - Dry the wafer using either compressed air or by spin-drying
 - Inspect the wafer under an upright light microscope at 50–100× magnification to ensure patterns have developed properly (Supplementary Fig. 1)

■ PAUSE POINT The developed wafer can be kept at RT in a dust-free environment indefinitely.

? TROUBLESHOOTING

- 8 Etch the wafer using a Bosch process in an AMS 100 I-Speeder to produce vertical pillars, then remove the remaining resist with O₂ plasma.
 - Clean the chamber of the inductively coupled plasma (ICP) reactive ion etcher for 20 min prior to beginning. Use O₂ gas set to 200 standard cubic centimeters per min (SCCM) with ICP power set to 1,800 W and biased power set to 60 W
 - Place the wafer in the etcher, and set the following parameters: wafer temperature = 10 °C, chamber pressure = 0.04 mbar, source-target distance = 200 mm
 - Etch the wafer using a Bosch process. The etching step is 200 SCCM SF₆ for 7 s with ICP power set to 2,000 W and capacitive coupled plasma power at 0 W. The passivation step is 80 SCCM C₄F₈ for 3 s with ICP power set to 2,000 W and capacitive coupled plasma power in chopped low-frequency bias mode: 80 W for 10 ms and 0 W for 90 ms. The etching time depends on the desired structure height (see Fig. 5d for guide)
 - Remove the resist with the AMS 100 I-speeder using O₂ gas at 200 SCCM for 10 min with the following parameters: wafer temperature = 10 °C, chamber pressure = 0.04 mbar, source-target distance = 200 mm, ICP power = 2,500 W with biased power = 50 W
- 9 Measure the height of the etched structures by moving the stylus of a DektakXT profilometer over the $1,000 \times 500 \mu\text{m}^2$ rectangle in the pattern.

- 10 Inspect the true widths of the pillars with an SEM.

■ PAUSE POINT The silicon wafer can be kept at RT indefinitely.

Passivation and dicing of the silicon micropillar wafer ● **Timing** ~12 h

- 11 Passivate the silicon micropillar wafer with a silane compound using vapor deposition.
 - Evacuate air in a glass desiccator with argon to remove moisture
 - Pipette 10 µL of (tridecafluoro-1,1,2,2-tetrahydrooctyl)trichlorosilane into a tube in the desiccator. Leave the tube open
 - Place the wafer in the desiccator. Pull vacuum in desiccator down to ~10 mbar
 - Close the desiccator valve, and turn off the vacuum
 - Remove wafer after ~12 h
- **PAUSE POINT** The silanized wafer can be kept at RT indefinitely.
- 12 (Optional) Split the wafer into four quarters by scratching with a diamond scribe. Since the wafers are made of a lattice crystal of silicon, they will break along a well-defined plane. For sample preparation and imaging procedure for VerCINI, proceed to Part 1 (Steps 13–33), or for µVerCINI proceed to Part 2 (Steps 34–68).

Part 1: VerCINI sample preparation and imaging

▲ **CRITICAL** Sample preparation and imaging protocols for VerCINI (Part 1) and µVerCINI (Part 2) are described separately. VerCINI imaging using cells immobilized in agarose cell traps (Part 1) is the more common use case, and is straightforward to implement. µVerCINI (Part 2) is more difficult due to more elaborate sample preparation and imaging, and reduced cell loading efficiency, and should only be attempted after users are experienced at standard VerCINI.

Preparation of VerCINI pads ● **Timing** ~20–40 min

- 13 Apply a Gene Frame to a microscope slide. Leave the plastic cover adhered to the Gene Frame that has a square hole in the middle.
- 14 Prepare 10 mL of 6% (wt/vol) agarose in growth medium (with any inducers required), and microwave until dissolved. Short bursts in the microwave with swirling in between allow bubbles to settle.
- 15 After agarose is fully dissolved, place the molten agarose in a 90 °C water bath for 5–10 min. Since the 6% molten agarose is very viscous, this will allow time for bubbles to migrate to the surface while not allowing the agarose to solidify.
- 16 Using wide-bore pipette tips (or cutting the ends off regular ones), apply 800 µL agarose to the center of the pillars (Figure 6a(i)).
- 17 Gently but firmly press the microscope slide on top of the agarose (Gene Frame down), aligning the micropillars with the center of the Gene Frame (Figure 6a(ii)). Keep the wafer with attached slide at the temperature at which cells will be imaged.
- **PAUSE POINT** Agarose pads should be left in place on the wafer at the imaging temperature until ready to load with cells.

? TROUBLESHOOTING**Loading cells into VerCINI pads** ● **Timing** ~10–20 min

▲ **CRITICAL** Steps 18–26 should be performed at a constant temperature as much as possible to avoid perturbations to cell physiology.

- 18 Centrifuge 0.5–1 mL of cell culture (OD₆₀₀ between 0.3 and 0.5) at 17,000 relative centrifugal force (RCF) for 1 min. Concentration and volume of cells added can be adjusted as required.
- 19 Remove supernatant, and resuspend in 8–15 µL prewarmed medium.
- 20 Using a scalpel, remove agarose slide from the micropillar wafer (Figure 6a(iii)). To do this, slide the scalpel between the agarose pad and the wafer, then use the scalpel to lever the agarose pad and slide it away from the wafer. Take care not to disturb the holes or to touch the nanofabricated pillars.
- **PAUSE POINT**
- 21 Place a 9 mm silicone gasket on top of the microholes, and spot the concentrated cell culture into the center (Figure 6a(iv)). To prevent evaporation, cover the gasket with a plastic slip and tape it down to the slide. For this, we commonly use the plastic coverslips supplied with Gene Frames, although many other similar covers are possible.
- 22 Tape the slide to a flat-bottomed centrifuge rotor with appropriate balance, and centrifuge at 3,220 RCF for 4 min (Figure 6a(iv)).
- **PAUSE POINT**
- 23 Wash off excess cells from the top of the pad by holding the pad near-vertically over a waste container (Figure 6a(v)) and slowly (1 mL/5 s) pipetting fresh, prewarmed medium onto the top of the agarose pad, allowing the medium to flow over the imprinted area and drop into the waste

container. Repeat this step at least five times until the majority of excess cells are removed (it is impossible to remove all of the cells, so some excess will still be visible by eye). This step is the most inconsistent, so it can be adjusted through trial and error. **▲CRITICAL STEP** If the washing step is not thorough enough, the pad will be covered in horizontal cells covering up the vertically immobilized cells (Fig. 6b). If the pad is washed too aggressively, the vertically immobilized cells will be flushed out of the microholes. The washing step is also important to maintain hydration of the pad after centrifugation.

- 24 Allow the pad to air dry until no excess liquid remains (~2 min).
- 25 Remove agarose outside the imprinted region by cutting around the imprinted region using a scalpel. This ensures sufficient oxygen supply to the cells once the coverslip is applied (Figure 6a(vi)).
- 26 Peel off the remaining plastic from the Gene Frame, and apply the coverslip. Ensure the coverslip is fully adhered to the Gene Frame by pressing down around all the edges.

Imaging with VerCINI ● **Timing** 10 min to 12 h

▲CRITICAL If doing live-cell imaging, Steps 27–33 should be done with a microscope that is surrounded by an incubation box preheated to the cell growth temperature. Failure to do so can result in temperature shock to the cells, compromising results.

- 27 Transport the slide to the microscope in a prewarmed empty pipette tip box to reduce temperature fluctuations in the sample.
- 28 Mount the slide on the microscope, preferably with a low-autofluorescence immersion oil such as Olympus Type-F.
- 29 Using bright-field illumination, identify an area of the VerCINI slide with a high loading efficiency and a low number of horizontal cells on top of the pad.

? TROUBLESHOOTING

- 30 Using fluorescence microscopy, take snapshots to scan the Z-plane to find the structure you wish to image. Keep the number of snapshots to a minimum to avoid photobleaching. It is often useful to take a Z-stack image of the entire cell to ensure the correct structure and plane are imaged.
- 31 Set focus lock to the optimal Z-plane.
- 32 Record a short bright-field time lapse as a control. This allows later identification of wobbling cells that can affect apparent protein dynamics. We recommend recording ~20 frames over ~1 s.
- 33 Record fluorescence with desired settings.

Part 2: μVerCINI sample preparation and imaging (advanced)

▲CRITICAL μVerCINI (Part 2) is more difficult than standard VerCINI (Part 1) owing to more elaborate sample preparation and imaging, and reduced cell loading efficiency, and should only be attempted after users are experienced at standard VerCINI.

Preparation of μVerCINI device ● **Timing** ~2 h

- 34 Make a 10:1 ratio of PDMS elastomer base:curing agent by mixing 10 g elastomer base and 1 g curing agent in a glass or plastic vessel, and stir vigorously.
- 35 Degas the mixture by placing it in a vacuum chamber and pulling vacuum for ~15 min.
- 36 Pour ~1 mL on top of the silicon micropillars (Figure 7a(i)).
- 37 Place a microscope coverslip on top, and press down gently but firmly with a marker cap or similar device with a flat face (Figure 7a(ii)). It is important to press down with enough force to produce a thin layer of PDMS between the pillars and the coverslip, but not so hard that the pillars may be damaged. Cover the back of the coverslip with some remaining PDMS. This will make it easier to remove some PDMS after baking.
- 38 Set the silicon wafer with PDMS and coverslip in an oven, and bake at 80 °C for 1–2 h.
- 39 Take the wafer out of the oven, and peel off the outer layer of PDMS covering and surrounding the coverslip. Use a flat-edged blade, such as the bare blade of a utility knife, to slide under and pull off the PDMS-covered coverslip (Figure 7a(iii)). Be very careful not to damage the pillars with the blade while doing this.

■PAUSE POINT After fabrication, μVerCINI coverslips can be stored at RT indefinitely.

? TROUBLESHOOTING

- 40 Drill two holes in a glass microscope slide ~15 mm apart diagonally using a power drill equipped with diamond drill bits. Use a small volume of water to prevent glass dust kicking up during drilling.

- 41 Clean the slide to remove glass dust and other impurities by sonicating in ethanol for 15 min and wiping with a tissue.
- 42 Using either a laser engraver or a blade, cut a groove in a piece of double-sided tape to form the flow channel. The channel must be long enough to reach the inlet and outlet holes, and wide enough in the center to accommodate the microhole array.
- 43 Adhere the piece of tape to the microscope slide so that the holes line up with the ends of the channel (Fig. 7b). Ensure that the tape seals well by pressing around all the edges. Do not remove the plastic covering from the other side of the tape.
- 44 Take two 10 µL pipette tips and cut them in half, keeping the thinnest end. Cut a further ~2–3 mm from the ends of the tips (where they are thinnest). We find this prevents the tips from protruding too far through the drilled holes and interfering with fluid flow.
- 45 Cut two polyethylene tubes for inlet and outlet tubing. We use 24 cm for the inlet and 67 cm for the outlet.
- 46 Insert the inlet and outlet tubing into the cut pipette tips (Fig. 7b), and epoxy them in place.
- 47 Insert the cut pipette tips into the drilled holes of the microscope slide on the opposite side from the double-sided tape (Fig. 7b). Ensure that they do not protrude through the holes. Seal the interface by spreading epoxy between the tip and slide.
- 48 Slide a needle into the outlet tubing entrance.

■ PAUSE POINT The microfluidic chamber top can be stored at RT indefinitely.

? TROUBLESHOOTING

Loading cells into µVerCINI coverslip ● Timing ~10–20 min

▲ CRITICAL Steps 49–57 should be performed at a constant temperature as much as possible to avoid perturbations to cell physiology.

- 49 Treat the PDMS-coated coverslip with air or oxygen plasma for 3 min (Figure 7c(i)). This treatment renders the PDMS hydrophilic for a relatively short time (a few hours), as material deeper in the PDMS will eventually migrate to the surface and render it hydrophobic again.
- 50 Centrifuge 0.5–1 mL of cell culture (OD_{600} between 0.3 and 0.5) at 17,000 RCF for 1 min. Concentration and volume of cells added can be adjusted as required.
- 51 Remove supernatant, and resuspend in 8–15 µL prewarmed medium.
- 52 Place a 9 mm diameter silicone gasket on top of the PDMS microholes, and spot the cell culture onto the holes (Figure 7c(ii)).
- 53 Place the coverslip on a flat-bottomed centrifuge rotor, and cover it with a hard plastic bottle cap taped down to the plate adapter to prevent liquid evaporation during centrifugation. Use an appropriate weight balance.
- 54 Centrifuge the cells into the holes for 4 min at 3,220 RCF (Figure 7c(iii)).
- 55 Remove the silicone gasket. Rinse off excess cells from the PDMS surface using medium by holding the coverslip upside down over a waste container and gently pipetting 1–2 mL medium over the surface (Figure 7c(iv)). The liquid on the PDMS surface should appear clear. If it remains turbid, rinse with more medium. **▲ CRITICAL STEP** If the washing step is not thorough enough, the surface will be covered in horizontal cells covering up the vertically immobilized cells (Fig. 6b). If the surface is washed too aggressively, the vertically immobilized cells will be flushed out of the microholes.

? TROUBLESHOOTING

- 56 Dab with a tissue to dry off the edges of the PDMS. Be careful not to dry off the region near the holes themselves. **▲ CRITICAL STEP** Ensure there is only a thin layer of liquid remaining on top of the holes. Too much liquid can result in a poorly sealed chamber as liquid spreads under the double-sided tape, but too little liquid runs the risk of dehydrating the cells.
- 57 Seal the chamber together by peeling off the plastic covering of the double-sided tape on the top of the flow chamber (Fig. 7d) and pressing the top of the fluidic chamber to the µVerCINI coverslip, ensuring that the groove in the tape is over the microholes (Fig. 7d). Seal the chamber fully by pressing around the edges of the tape.

Imaging with µVerCINI ● Timing 10 min to 12 h

▲ CRITICAL If doing live-cell imaging, Steps 58–68 should be done with a microscope that is surrounded by an incubation box preheated to the cell growth temperature. Failure to do so can result in temperature shock to the cells, compromising results.

- 58 Transport the slide to the microscope in a prewarmed empty pipette tip box to reduce temperature fluctuations in the sample.

- 59 Make sure the high-working-distance objective is inserted, and use the appropriate immersion oil.
- 60 Position the μ VerCINI device above the objective. Place reservoirs of medium inside the microscope incubation box, and place the inlet tubing into one of them. Connect the needle of the outlet tubing to a 20 mL syringe. Attach the syringe to the syringe pump.
- 61 Fill the chamber with medium using the syringe pump operating in Withdraw mode using the following settings: diameter = 6", flow rate = 10 mL/s. Ensure medium has flowed into the chamber (~10 s). By operating in Withdraw mode, any failure to seal the chamber will result in the syringe pump pulling air. This is preferable to operating in Infuse mode, where failure to seal the chamber can result in messy leaks in the microscope body.

? TROUBLESHOOTING

- 62 Change flow rate to something lower (e.g., 1.1 mL/s) for a slower, steady flow.
- 63 Using bright-field illumination, identify an area of the μ VerCINI slide with a high loading efficiency and a low number of horizontal cells on top of the PDMS.

? TROUBLESHOOTING

- 64 Using fluorescence microscopy, take snapshots to scan the Z-plane to find the structure you wish to image.
- 65 Use an autofocus method of choice to maintain focus lock. We use an image-based system using a separate infrared bright-field pathway with a custom Micro-Manager plugin¹², although other methods may be applied.
- 66 Record a short bright-field time lapse as a control. This allows later identification of wobbling cells that can affect apparent protein dynamics. We recommend recording ~20 frames over ~1 s.
- 67 Record fluorescence with desired settings.
- 68 To change fluids during imaging, move the inlet tubing from one reservoir to another.

? TROUBLESHOOTING

Image processing and analysis for VerCINI and μ VerCINI ● Timing 30 min to 2 h

▲ CRITICAL The following image processing and analysis steps can be used with both VerCINI and μ VerCINI.

- 69 Select cells that are suitable for subsequent analysis by inspecting raw TIF files in Fiji or ImageJ.
 - If a bright-field video was saved, exclude poorly trapped cells (these will appear to wobble in the holes owing to diffusion). If the sample has been characterized previously, poorly trapped cells can be removed using the fluorescence video
 - If a fluorescence Z-stack was saved, exclude cells where signal is not at the correct Z-plane
- 70 Produce videos of cropped, denoised rings using the VerciniAnalysisJ Action Bar.
 - Draw a 60 × 60 pixel ROI around each usable cell, and record the position in the ImageJ ROI Manager. Click ‘Save ROIs’ to create a compressed folder containing positions of identified cells in the same directory as the TIF file
 - Click ‘Batch denoise+register+crop’, and select the directory containing the TIF and zip files. The output will be a denoised and registered TIF file of the full FoV and a folder called ‘Indiv_rings’ containing each cell cropped to the selected ROI. Note: the denoising step may take some time (>0.5 h) for large datasets
- 71 Subtract the cytoplasmic backgrounds and produce circumferential kymographs using the testVerciniAnalysis script in MATLAB.
 - Copy and paste the file testVerciniAnalysis.m from the directory ring-fitting2/testing into the Indiv_rings folder
 - Open testVerciniAnalysis.m in MATLAB, and change any options as required, especially the fname variable defining the files you want to analyze. More information about options can be found in the documentation in the GitHub repository. Detailed documentation of all the optional arguments to the VerCINI software may be accessed by typing ‘doc verciniAnalysis’ or ‘doc manualVerciniAnalysis’ in MATLAB. As the VerCINI circle-fitting method is performed on a per-frame basis, the analysis method works equally well on septa that constrict noticeably over the data acquisition period. In this case, analysis of constriction rate can also be performed as the cell radius for each frame is returned as a parameter of the analysis
 - Run the testVerciniAnalysis script. A new directory, Indiv_rings/analysed, is created containing the kymograph (with and without background subtraction) and the background-subtracted VerCINI movie

Kymograph analysis ● Timing ~5–15 min

- 72 Manually trace individual tracks in kymographs using VerciniAnalysisJ Action Bar in Fiji or ImageJ.
- Open the ‘_KymoRawWrap.tif’ images to analyze
 - (Optional) Use ‘Ridge Filter’ in the Action Bar to highlight ridges in the image
 - For each image, use the straight line tool to trace over the kymograph lines and add the trace to the ROI manager
 - Click ‘save ROIs’ to create a compressed folder containing the traced lines in the same directory as the TIF file
- 73 Once all of the kymographs have been traced, click ‘Batch kymotrace statistics’.
- Define the camera pixel size and the frame interval of the images, then select the folder containing the TIF files and compressed ROI files. The results are output in a new ImageJ window and can be saved as a .csv file

Troubleshooting

Troubleshooting advice can be found in Table 1.

Table 1 | Troubleshooting table

Step	Problem	Possible reason	Solution
2	The output from BEAMER is a row/column of squares rather than a full array	The loops in series performing the translations are only keeping the final loop iteration	Change loop options to merge results of all iterations, and repeat
4	The wafer is not uniformly covered with resist	Bubbles in the resist streaked across the wafer	Remove the resist layer by washing the wafer with acetone, and repeat the spin-coating, careful to remove bubbles
7	There is still resist in unpatterned regions All resist was dissolved after development	The wafer was not developed long enough The wafer was not baked after the pattern was written	Develop the wafer for another ~30 s in MF-321, soak in water, and dry Repeat the resist coating, writing and development (Steps 4–7)
17	The agarose pad is too thick or uneven	The agarose pad solidified too quickly as the microscope slide was pressed down on the wafer	Discard slide. Repeat Steps 13–17. Perform Step 17 on top of a hotplate set to 50 °C. The higher temperature will give more time for the agarose to solidify while pressing down
20	The agarose pad stuck to the wafer after removing the slide	—	Carefully peel the pad off the wafer and set it inside the Gene Frame with holes facing up
22	Cell culture is a dried smear on the pad	Cell culture dried out during centrifugation	Discard pad. Repeat Steps 13–22 with fresh pad, using a silicone gasket to hold the culture in place and a plastic cover to prevent evaporation
29	There are too many horizontal cells on the pad There are too few cells loaded into holes	Cells were not washed off sufficiently after loading Cells were washed off too aggressively after loading Cell culture was not concentrated enough Hole widths are too small for cells	Discard slide. Repeat Steps 13–29, using extra medium to wash off unloaded cells Discard slide. Repeat Steps 13–29, being extra gentle with rinsing off unloaded cells Discard slide. Repeat Steps 13–29, taking care to concentrate cell culture ~100× before spotting on pad Search for a region of the pad with a larger hole size
39	Most cells are wobbling in the holes PDMS will not peel off the silicon wafer The coverslip breaks when peeling it off of wafer PDMS comes off silicon wafer easily, but will not come off back of coverslip	Hole widths are too large for cells The desiccator lost vacuum during the silanization step, no passivation occurred Elastomer base: curing agent ratio was too high Elastomer base: curing agent ratio was too low	Search for a region of the pad with a smaller hole size Try to carefully remove the PDMS and repeat the silanization (Step 11) Try to carefully remove the coverslip and repeat Steps 34–39 with lower ratio Discard the PDMS-covered coverslip, and repeat Steps 34–39 with higher ratio
48	The needle punctures the tubing	The needle is being pushed while the tip is catching the inside wall of the tubing	Cut off the punctured segment of tubing. Repeat while bending the tubing away from the needle tip to avoid it catching the inside wall

Table continued

Table 1 (continued)

Step	Problem	Possible reason	Solution
55	Cell culture is a dried smear on the PDMS	Cell culture dried out during centrifugation	Discard coverslip. Repeat Steps 34–39, then Steps 49–55, careful to use a silicone gasket to hold the culture in place and a plastic lid to prevent evaporation
61	The chamber does not fill with medium	The chamber is not sealed properly due to liquid under the tape	Discard the device. Repeat Steps 34–61 with a fresh device and taking care to dry the PDMS outside the hole pattern in Step 56 prior to sealing with tape
		The cut pipette tips are pressed against the PDMS and obstructing flow	Discard the device. Repeat Steps 34–61, careful to cut a few millimeters from the ends of pipette tips before inserting into drilled holes (Step 44)
63	There are too many horizontal cells on the PDMS	Cells were not washed off sufficiently after loading	Flush medium through with a high flow rate for ~10 s to dislodge horizontal cells. Otherwise, discard the device and repeat Steps 34–63
	The holes are filled with air bubbles rather than cells	The PDMS is too hydrophobic	Discard the device. Repeat Steps 34–63, careful to treat the PDMS-coated coverslip with plasma (Step 49) before loading cells
	There are too few cells loaded into holes	Cells were washed off too aggressively after loading Cell culture was not concentrated enough	Discard device. Repeat Steps 34–63, being extra gentle with rinsing off unloaded cells Discard device. Repeat Steps 34–63, taking care to concentrate cell culture ~100× before spotting on PDMS
	Most cells are wobbling in the holes	Hole widths are too small for cells Hole widths are too large for cells	Search for a region of the PDMS with a larger hole size Search for a region of the PDMS with a smaller hole size
68	Air is being pulled over tops of cells rather than liquid medium	The reservoir of medium is empty The inlet tubing is not in the medium reservoir	Stop imaging. Discard device. Repeat Steps 34–68 using larger reservoir of medium and/or lower flow rate Stop imaging. Discard device. Repeat Steps 34–68, careful that inlet tubing is resting at bottom of reservoir during imaging

Timing

Silicon wafer fabrication total (Steps 1–12): ~16 h

Steps 1–3, design of an array-of-squares pattern: 30 min to 2 h, depending on speed of user

Steps 4–10, fabrication of a silicon micropillar wafer: ~3 h

Steps 11–12, passivation and dicing of the silicon micropillar wafer: ~12 h

Part 1: VerCINI total (Steps 13–33): 40 min to 12 h

Steps 13–17, preparation of VerCINI pads: ~20–40 min

Steps 18–26, loading cells into VerCINI pads: ~10–20 min

Steps 27–33, imaging with VerCINI: 10 min to 12 h

Part 2: μVerCINI total (Steps 34–68): ~2–12 h

Steps 34–48, preparation of μVerCINI device: ~2 h

Steps 49–57, loading cells into μVerCINI coverslip: ~10–20 min

Steps 58–68, imaging with μVerCINI: 10 min to 12 h

Analysis total (Steps 69–73): ~30 min – 2 h

Steps 69–71, image processing and analysis: 30 min to 2 h, depending on size of dataset

Steps 72–73, kymograph analysis: ~5–15 min

Anticipated results

We have provided a detailed protocol for imaging vertically confined bacterial cells using both VerCINI and μVerCINI. Using these methods, structures and biomolecular dynamics along the short axes of bacterial cells can be observed with high resolution without any special requirements for fluorophores or imaging modalities. VerCINI methods can also be combined with a wide range of other imaging methods (e.g., SIM or STORM) to provide greater resolution than is possible with each method individually.

Examples of results that a researcher can expect to obtain from VerCINI can be seen in Figs. 1 and 2. With VerCINI, the treadmilling dynamics of the bacterial division protein FtsZ can be imaged with higher sensitivity than any other approach to date¹² (Fig. 1). Beyond this, VerCINI has also been used to track single molecules of both elongosome and divisome proteins moving circumferentially around the cell for minutes (ref. ¹⁶ and our unpublished results) and to image the constricting division septum using STORM (ref. ¹⁷ and our unpublished results). VerCINI also makes it possible to image cell pole proteins like TlpA at high resolution and SNR (Fig. 2), paving the way for super-resolution studies to reveal the spatial organization of these regions with unprecedented detail.

If researchers choose to use μVerCINI to image cells during antibiotic perturbations, they can expect to obtain results similar to those shown in Fig. 3. We have used μVerCINI to observe the rapid effect of the FtsZ-targeting antibiotic PC190723 on FtsZ treadmilling dynamics across all stages of cell division. However, μVerCINI is compatible with many other experimental designs that include imaging during continual fluid flow or fluid exchange. This can include chemostatic growth³⁴, live-to-fixed cell imaging³⁵ or DNA-PAINT (DNA point accumulation for imaging in nanoscale topography)³⁶.

Light microscopy of bacteria provides a wealth of information about their organization, but conventional imaging approaches are limited to viewing bacteria along their long axes only. VerCINI provides a complementary approach by orienting bacteria vertically and imaging along their short axes, substantially improving the imaging of many biologically important structures and dynamic processes in nonspherical bacteria that were previously difficult to observe. VerCINI has already found multiple applications in high-resolution imaging of bacterial spatial organization in the hands of a small number of early-adopter laboratories^{5,12,13,15–17}. We hope that the methods and protocols presented here will allow many other laboratories to use VerCINI to look at diverse questions in bacterial cell biology from a different angle.

Reporting Summary

Further information on research design is available in the Nature Research Reporting Summary linked to this article.

Data availability

Source data for all figures presented in the paper are available at figshare (<https://doi.org/10.25405/data.ncl.c.5652010.v1>).

Code availability

Custom software is available on the Holden lab GitHub page or Zenodo: https://github.com/HoldenLab/VerCINI_nanofab²⁵, <https://github.com/HoldenLab/DeepAutoFocus>³⁷, <https://github.com/HoldenLab/VerciniAnalysis>³⁸ and <https://github.com/HoldenLab/ring-fitting2>³⁰.

References

1. Huang, B., Babcock, H. & Zhuang, X. Breaking the diffraction barrier: super-resolution imaging of cells. *Cell* **143**, 1047–1058 (2010).
2. Pasquina-Lemonche, L. et al. The architecture of the Gram-positive bacterial cell wall. *Nature* **582**, 294–297 (2020).
3. Garner, E. C. et al. Coupled, circumferential motions of the cell wall synthesis machinery and MreB filaments in *B. subtilis*. *Science* **333**, 222–225 (2011).
4. Domínguez-Escobar, J. et al. Processive movement of MreB-associated cell wall biosynthetic complexes in bacteria. *Science* **333**, 225–228 (2011).
5. Bisson-Filho, A. W. et al. Treadmilling by FtsZ filaments drives peptidoglycan synthesis and bacterial cell division. *Science* **355**, 739–743 (2017).
6. Yang, X. et al. GTPase activity-coupled treadmilling of the bacterial tubulin FtsZ organizes septal cell wall synthesis. *Science* **355**, 744–747 (2017).
7. Kirkpatrick, C. L. & Viollier, P. H. Poles apart: prokaryotic polar organelles and their spatial regulation. *Cold Spring Harb. Perspect. Biol.* **3**, a006809–a006809 (2011).
8. Kuwada, N. J., Traxler, B. & Wiggins, P. A. Genome-scale quantitative characterization of bacterial protein localization dynamics throughout the cell cycle. *Mol. Microbiol.* **95**, 64–79 (2015).
9. Laloux, G. & Jacobs-Wagner, C. How do bacteria localize proteins to the cell pole? *J. Cell Sci.* <https://doi.org/10.1242/jcs.138628> (2014).
10. Surovtsev, I. V. & Jacobs-Wagner, C. Subcellular organization: a critical feature of bacterial cell replication. *Cell* **172**, 1271–1293 (2018).

11. Bowman, G. R., Lyuksyutova, A. I. & Shapiro, L. Bacterial polarity. *Curr. Opin. Cell Biol.* **23**, 71–77 (2011).
12. Whitley, K. D. et al. FtsZ treadmilling is essential for Z-ring condensation and septal constriction initiation in *Bacillus subtilis* cell division. *Nat. Commun.* **12**, 2448 (2021).
13. Perez, A. J. et al. Movement dynamics of divisome proteins and PBP2x:FtsW in cells of *Streptococcus pneumoniae*. *Proc. Natl Acad. Sci. USA* **116**, 3211–3220 (2019).
14. Chai, Y., Norman, T., Kolter, R. & Losick, R. An epigenetic switch governing daughter cell separation in *Bacillus subtilis*. *Genes Dev.* **24**, 754–765 (2010).
15. Söderström, B., Chan, H., Shilling, P. J., Skoglund, U. & Daley, D. O. Spatial separation of FtsZ and FtsN during cell division. *Mol. Microbiol.* **107**, 387–401 (2018).
16. McCausland, J. W. et al. Treadmilling FtsZ polymers drive the directional movement of sPG-synthesis enzymes via a Brownian ratchet mechanism. *Nat. Commun.* **12**, 609 (2021).
17. Trouve, J. et al. Nanoscale dynamics of peptidoglycan assembly during the cell cycle of *Streptococcus pneumoniae*. *Curr. Biol.* <https://doi.org/10.1016/j.cub.2021.04.041> (2021).
18. Bakshi, S., Choi, H. & Weisshaar, J. C. The spatial biology of transcription and translation in rapidly growing *Escherichia coli*. *Front. Microbiol.* **6**, 636 (2015).
19. Zhou, Z. et al. The contractile ring coordinates curvature-dependent septum assembly during fission yeast cytokinesis. *Mol. Biol. Cell* **26**, 78–90 (2015).
20. Thiagarajan, S., Munteanu, E. L., Arasada, R., Pollard, T. D. & O’Shaughnessy, B. The fission yeast cytokinetic contractile ring regulates septum shape and closure. *J. Cell Sci.* <https://doi.org/10.1242/jcs.166926> (2015).
21. Wollrab, V., Thiagarajan, R., Wald, A., Kruse, K. & Riveline, D. Still and rotating myosin clusters determine cytokinetic ring constriction. *Nat. Commun.* **7**, 11860 (2016).
22. Strahl, H. et al. Transmembrane protein sorting driven by membrane curvature. *Nat. Commun.* **6**, (2015).
23. Briegel, A. et al. New insights into bacterial chemoreceptor array structure and assembly from electron cryotomography. *Biochemistry* **53**, 1575–1585 (2014).
24. Deshpande, S. & Dekker, C. On-chip microfluidic production of cell-sized liposomes. *Nat. Protoc.* **13**, 856–874 (2018).
25. Whitley, K. VerCINI_nanofab. Zenodo <https://doi.org/10.5281/ZENODO.5548030> (2021).
26. de Jong, I. G., Beilharz, K., Kuipers, O. P. & Veening, J.-W. Live cell imaging of *Bacillus subtilis* and *Streptococcus pneumoniae* using automated time-lapse microscopy. *J. Vis. Exp.* **53**, e3145 (2011).
27. Ellefson, K. L., Dynes, J. L. & Parker, I. Spinning-spot shadowless TIRF microscopy. *PLoS ONE* **10**, e0136055 (2015).
28. McGorty, R., Kamiyama, D. & Huang, B. Active microscope stabilization in three dimensions using image correlation. *Opt. Nanoscopy* **2**, 3 (2013).
29. Schindelin, J. et al. Fiji: An open-source platform for biological-image analysis. *Nat. Methods* **9**, 676–682 (2012).
30. Holden, S. & Whitley, K. HoldenLab/ring-fitting2: v1.1.2.1. Zenodo <https://doi.org/10.5281/ZENODO.4570259> (2021).
31. Luisier, F., Vonesch, C., Blu, T. & Unser, M. Fast interscale wavelet denoising of Poisson-corrupted images. *Signal Process* **90**, 415–427 (2010).
32. Thevenaz, P., Ruttmann, U. E. & Unser, M. A pyramid approach to subpixel registration based on intensity. *IEEE Trans. Image Process* **7**, 27–41 (1998).
33. Jakobs, M. A., Dimitracopoulos, A. & Franze, K. KymoButler, a deep learning software for automated kymograph analysis. *eLife* **8**, e42288 (2019).
34. Wang, P. et al. Robust growth of *Escherichia coli*. *Curr. Biol.* **20**, 1099–1103 (2010).
35. Tam, J. et al. A microfluidic platform for correlative live-cell and super-resolution microscopy. *PloS ONE* **9**, e115512 (2014).
36. Almada, P. et al. Automating multimodal microscopy with NanoJ-Fluidics. *Nat. Commun.* **10**, 1223 (2019).
37. Whitley, K. D. et al. DeepAutoFocus. Zenodo <https://doi.org/10.5281/ZENODO.4573121> (2021).
38. Holden, S. HoldenLab/VerciniAnalysisJ: v1.1.1. Zenodo <https://doi.org/10.5281/ZENODO.4617277> (2021).
39. Erratum for the Report: "Treadmilling by FtsZ filaments drives peptidoglycan synthesis and bacterial cell division" by A. W. Bisson-Filho, Y.-P. Hsu, G. R. Squyres, E. Kuru, F. Wu, C. Jukes, Y. Sun, C. Dekker, S. Holden, M. S. VanNieuwenhze, Y. V. Brun, E. C. GarnerErratum for the Report: "Treadmilling by FtsZ filaments drives peptidoglycan synthesis and bacterial cell division". *Science* **367**, eaba6311 (2020).
40. Tinevez, J.-Y. et al. TrackMate: an open and extensible platform for single-particle tracking. *Methods* **115**, 80–90 (2017).

Acknowledgements

We acknowledge S. Pud (TU Delft; now at Twente) for help with wafer design and nanofabrication, S. Deshpande (TU Delft; now at Wageningen) for help with nanofabrication and soft lithography, M. Zuidam (TU Delft) for help with wafer etching, H. Strahl (Newcastle) for strains and helpful discussions, and J. Fritzsche (ConScience AB, Sweden) for helpful discussions. S.H., K.D.W., C.J. and S.M. acknowledge funding support by a Wellcome Trust & Royal Society Sir Henry Dale Fellowship [206670/Z/17/Z]. C.D. acknowledges funding support by the ERC Advanced Grants [883684] and [669598], and the NanoFront and BaSyC programs. S.M. is supported by a UK Biotechnology and Biological Sciences Research Council doctoral studentship.

Author contributions

K.D.W., S.M. and C.J. performed the experiments. K.D.W., S.M., S.H. and C.D. wrote the paper.

Competing interests

The authors declare no competing interests.

Additional information

Supplementary information The online version contains supplementary material available at <https://doi.org/10.1038/s41596-021-00668-1>.

Correspondence and requests for materials should be addressed to Kevin D. Whitley or Séamus Holden.

Peer review information *Nature Protocols* thanks Cecile Morlot and the other, anonymous, reviewer(s) for their contribution to the peer review of this work.

Reprints and permissions information is available at www.nature.com/reprints.

Publisher's note Springer Nature remains neutral with regard to jurisdictional claims in published maps and institutional affiliations.

Received: 26 July 2021; Accepted: 19 November 2021;

Published online: 31 January 2022

Related links**Key references using this protocol**

Bisson-Filho, A. W. et al. *Science* **355**, 739–743 (2017): <https://doi.org/10.1126/science.aak9973>

Perez, A. J. et al. *Proc. Natl. Acad. Sci. USA* **116**, 3211–3220 (2019): <https://doi.org/10.1073/pnas.1816018116>

Whitley, K. D. et al. *Nat. Commun.* **12**, 2448 (2021): <https://doi.org/10.1038/s41467-021-22526-0>

Reporting Summary

Nature Research wishes to improve the reproducibility of the work that we publish. This form provides structure for consistency and transparency in reporting. For further information on Nature Research policies, see our [Editorial Policies](#) and the [Editorial Policy Checklist](#).

Statistics

For all statistical analyses, confirm that the following items are present in the figure legend, table legend, main text, or Methods section.

n/a Confirmed

- The exact sample size (n) for each experimental group/condition, given as a discrete number and unit of measurement
- A statement on whether measurements were taken from distinct samples or whether the same sample was measured repeatedly
- The statistical test(s) used AND whether they are one- or two-sided
Only common tests should be described solely by name; describe more complex techniques in the Methods section.
- A description of all covariates tested
- A description of any assumptions or corrections, such as tests of normality and adjustment for multiple comparisons
- A full description of the statistical parameters including central tendency (e.g. means) or other basic estimates (e.g. regression coefficient) AND variation (e.g. standard deviation) or associated estimates of uncertainty (e.g. confidence intervals)
- For null hypothesis testing, the test statistic (e.g. F , t , r) with confidence intervals, effect sizes, degrees of freedom and P value noted
Give P values as exact values whenever suitable.
- For Bayesian analysis, information on the choice of priors and Markov chain Monte Carlo settings
- For hierarchical and complex designs, identification of the appropriate level for tests and full reporting of outcomes
- Estimates of effect sizes (e.g. Cohen's d , Pearson's r), indicating how they were calculated

Our web collection on [statistics for biologists](#) contains articles on many of the points above.

Software and code

Policy information about [availability of computer code](#)

Data collection

Microscopy data collected using Micro-Manager (versions 1.4beta and 2.0gamma).

Custom Micro-Manager plugin for autofocusing is available on the Holden lab Github page: <https://github.com/HoldenLab/DeepAutoFocus>.

Data analysis

Videos analysed using Fiji (v1.53) with open-source plugins PureDenoise, StackReg, and TrackMate (v6.0.1); and custom code available on the Holden lab Github page: <https://github.com/HoldenLab/VerciniAnalysis>.

Further data analysis done using Matlab with custom code available on the Holden lab Github page:
<https://github.com/HoldenLab/ring-fitting2>.

For manuscripts utilizing custom algorithms or software that are central to the research but not yet described in published literature, software must be made available to editors and reviewers. We strongly encourage code deposition in a community repository (e.g. GitHub). See the Nature Research [guidelines for submitting code & software](#) for further information.

Data

Policy information about [availability of data](#)

All manuscripts must include a [data availability statement](#). This statement should provide the following information, where applicable:

- Accession codes, unique identifiers, or web links for publicly available datasets
- A list of figures that have associated raw data
- A description of any restrictions on data availability

All source data for figures and results in this paper can be found in the Figshare repository: <https://doi.org/10.25405/data.ncl.c.5652010.v1>

Field-specific reporting

Please select the one below that is the best fit for your research. If you are not sure, read the appropriate sections before making your selection.

Life sciences Behavioural & social sciences Ecological, evolutionary & environmental sciences

For a reference copy of the document with all sections, see nature.com/documents/nr-reporting-summary-flat.pdf

Life sciences study design

All studies must disclose on these points even when the disclosure is negative.

Sample size	No a priori sample size calculations were performed. No specific sample size was chosen, as the number of pillars per wafer, and the number of microholes per FoV meant a moderate to large sample size for each measurement, and were sufficiently large for robust statistical analysis.
Data exclusions	No data was excluded.
Replication	The number of independent replicates for any new results, defined as the number of experiments done using independently-prepared samples (e.g. wafers), is described where the results appear.
Randomization	Allocating experimental groups was not relevant for this study, as all bacterial cells of a particular strain are genetic clones.
Blinding	Blinding was neither possible nor necessary for this study, as 1) all bacterial cells of a particular strain are genetic clones and 2) analyses were not sufficiently subjective to require researcher blinding.

Reporting for specific materials, systems and methods

We require information from authors about some types of materials, experimental systems and methods used in many studies. Here, indicate whether each material, system or method listed is relevant to your study. If you are not sure if a list item applies to your research, read the appropriate section before selecting a response.

Materials & experimental systems

- | | |
|-------------------------------------|--|
| n/a | Involved in the study |
| <input checked="" type="checkbox"/> | <input type="checkbox"/> Antibodies |
| <input checked="" type="checkbox"/> | <input type="checkbox"/> Eukaryotic cell lines |
| <input checked="" type="checkbox"/> | <input type="checkbox"/> Palaeontology and archaeology |
| <input checked="" type="checkbox"/> | <input type="checkbox"/> Animals and other organisms |
| <input checked="" type="checkbox"/> | <input type="checkbox"/> Human research participants |
| <input checked="" type="checkbox"/> | <input type="checkbox"/> Clinical data |
| <input checked="" type="checkbox"/> | <input type="checkbox"/> Dual use research of concern |

Methods

- | | |
|-------------------------------------|---|
| n/a | Involved in the study |
| <input checked="" type="checkbox"/> | <input type="checkbox"/> ChIP-seq |
| <input checked="" type="checkbox"/> | <input type="checkbox"/> Flow cytometry |
| <input checked="" type="checkbox"/> | <input type="checkbox"/> MRI-based neuroimaging |